UNIVERSIDAD DE CHILE
FACULTAD DE CIENCIAS FÍSICAS Y MATEMÁTICAS
DEPARTAMENTO DE INGENIERÍA MECÁNICA

STUDY OF HYDROGEN GLOBAL MARKET AND TECHNICAL AND ECONOMIC PREFEASIBILITY OF USING THE PROTON EXCHANGE MEMBRANE FUEL CELL (PEM) FUELED WITH HYDROGEN IN CHILEAN MINING MOBILITY

MEMORIA PARA OPTAR AL TÍTULO DE
INGENIERA CIVIL MECÁNICA

CAMILA ANDREA NIÑO VEGA

PROFESOR GUÍA:
WILLIAMS CALDERÓN MUÑOZ

MIEMBROS DE LA COMISIÓN:
PAULINA RAMÍREZ DEL BARRIO
KOEN LANGIE

SANTIAGO DE CHILE
NOVIEMBRE 2020

RESUMEN DE LA MEMORIA PARA OPTAR AL
TÍTULO DE INGENIERA CIVIL MECANICA
POR: CAMILA ANDREA NIÑO VEGA
FECHA: NOVIEMBRE 2020
PROF. GUÍA: WILLIAMS CALDERÓN MUÑOZ

ESTUDIO DEL MERCADO GLOBAL DE HIDRÓGENO Y ANÁLISIS DE PREFACTIBILIDAD TÉCNICA Y ECONÓMICA DEL USO DE LA CELDA DE COMBUSTIBLE TIPO MEMBRANA DE INTERCAMBIO PROTÓNICO (PEM) ALIMENTADA CON HIDRÓGENO EN TRANSPORTE EN LA MINERÍA CHILENA

La crisis climática es palpable: según Naciones Unidas, tormentas, incendios forestales, sequías y otros fenómenos meteorológicos extremos, alimentados por el cambio climático, han afectado a 4.500 millones de personas en los últimos 20 años. Siendo el costo de estos desastres, sólo en 2018, de 160 billones de dólares. Las constantes emisiones globales de gases efecto invernadero provocan el suceso de desastres meteorológicos gracias al violento aumento de las temperaturas anuales en la atmósfera terrestre, por encima de los niveles preindustriales; fenómeno denominado efecto invernadero. La progresión del efecto invernadero ha motivado la creación de políticas energéticas en todo el mundo. En una economía dominada por la demanda de combustibles fósiles, la descarbonización de sectores como la industria termoeléctrica, la calefacción, el gas o la movilidad se realiza en gran medida por separado. Para alcanzar la meta por ser carbono neutral a mediados de siglo, los sectores industriales deben integrarse para proporcionar energía renovable desde el sector eléctrico hacia los demás sectores. Para lograr el acoplamiento sectorial, el Hidrógeno se perfila como el candidato energético ideal que podría unificar los sectores mediante la electrificación de la matriz energética. Dentro de este informe, se describe el comportamiento del mercado internacional del Hidrógeno, las propiedades del Hidrógeno, sus métodos de producción y las tecnologías alimentadas con Hidrógeno. Se estudia el estado actual e industrialización del mercado internacional de pilas de combustible hidrogenadas para evaluar la viabilidad de introducir está tecnología a Hidrógeno para movilidad en la minería a cielo abierto de Chile.

La minería ha sido tradicionalmente un sector difícil de descarbonizar. Las minas suelen utilizar motores Diésel, emisores de gases efecto invernadero, para alimentar generadores de respaldo, cargadores, grandes camiones y otros vehículos. Para mejorar la huella de carbono de las soluciones existentes, algunas empresas mineras están tomando medidas para adoptar tecnologías carbono neutrales, como las pilas de combustible a Hidrógeno. Para demostrar el uso de las pilas de combustible en aplicaciones mineras, se realiza una prefactibilidad técnica y económica de un camión de extracción minero equipado con una pila de combustible a Hidrógeno y una batería. Con el reequipamiento del Komatsu 930E-4, el propósito es el reemplazo del motor Diésel por una pila de combustible. Por tanto, la prefactibilidad técnica y económica se realiza mediante la comparación entre el camión adaptado en su tren de potencia con una pila de combustible a Hidrógeno y una Batería Ion-Litio y el camión convencional equipado en su tren de potencia con un motor Diésel de combustión interna. De la evaluación se concluye que la introducción de celdas de combustible alimentadas con Hidrógeno en movilidad para la minería a cielo abierto en Chile aún no es una solución económicamente viable al 2020 dado sus altos costos de manufactura de la pila de celda de combustible PEM y de producción de Hidrógeno. Sin embargo, sí resulta técnica y económicamente viable invertir en CAEX a pilas de combustible hidrogenadas en vez de CAEX a motor Diésel al 2030, dada la reducción de costos de energía y manufactura.

ABSTRACT OF THE THESIS TO QUALIFY
FOR MECHANICAL ENGINEERING DEGREE
BY CAMILA ANDREA NIÑO VEGA
DATE: AUGUST 2020
TUTOR: WILLIAMS CALDERÓN MUÑOZ

STUDY OF HYDROGEN GLOBAL MARKET AND TECHNICAL AND ECONOMIC PREFEASIBILITY OF USING THE PROTON EXCHANGE MEMBRANE FUEL CELL (PEM) FUELED WITH HYDROGEN IN CHILEAN MINING MOBILITY

The climate crisis is palpable: According to the United Nations, storms, forest fires, droughts and other extreme weather events fueled by climate change have affected 4.5 billion people in the last 20 years. Moreover, a study by the company of German insurance Munich RE showed that the cost of these disasters in 2018 alone amounted to US $ 160 billion. The continuing projections of damage caused by the emission of greenhouse gases are terrible and incalculable. The greenhouse effect has become the deciding factor for energy policies around the world. In an economy dominated by the demand for fossil fuels, the decarbonization of sectors such as industry, energy, heating, gas or mobility was largely carried out separately. To reach the goal of zero emissions by mid-century, the industrial sectors must be integrated to provide renewable energy from the electricity sector to support the decarbonization. This sectoral coupling is a fundamental element of the energy transition. To achieve the coupling of all industrial sectors, Hydrogen is emerging as the ideal energy candidate which could potentially unite the different sectors through the electrification of the energy matrix. In this report the current state of the international Hydrogen market is described in order to understand its properties, the growth of the market together with the production methods and technologies fueled with Hydrogen. Specifically, the current state and industrialization of the international market for hydrogen fuel cells are studied to evaluate the viability of introducing hydrogen fuel cells in mobility at Chilean open-pit mining.

The mining and materials extraction industry has traditionally been a sector that is difficult to decarbonize. Mines commonly utilize polluting diesel engines to power backup generators, loaders, large material handling trucks, and other vehicles. To improve the carbon footprint of existing solutions, some mining companies are taking steps to adopt zero-emission technologies such as hydrogen fuel cells. To demonstrate fuel cell use in mining applications, in this report a technical and economic pre-feasibility of an ultra-heavy-duty mining truck retrofitting with hydrogen fuel cell and battery is carried out. With the haul truck retrofitting the purpose is the Diesel engine replacement by zero-emission fuel cell. Therefore, the technical and economic pre-feasibility is realized through the comparison between the truck adapted with hydrogen fuel cell and battery and the conventional truck equipped with an internal combustion diesel engine.

The evaluation has concluded that the introduction of mobile hydrogen fuel cells in Chilean open-pit mining cannot be an economically viable solution in 2020, due to the high capital and energy costs. However, the haul truck retrofitted with hydrogen fuel cell and battery is technically more efficient and has lower long-term operating and owning costs by 2030. Therefore, by 2030 it will be both technically and economically more viable to invest in H2 PEMFC for truck retrofitting than to invest in Diesel engines for conventional trucks.

Dedicado a mis padres Gerardo y Marcela, a mi hermana Paulina y a mis abuelitos Rubén y Rosa

AGRADECIMIENTOS

Empezando por agradecer a mis padres, Marcela y Gerardo, quienes siempre me han alentado, siendo mi principal motivación. Lo más valioso que pudieron haberme dado es la educación que hoy tengo. Espero tenerlos siempre conmigo.

A mi hermana Paulina, quien día a día me enseña a ser mejor persona y con quien siempre he podido compartirlo todo. Agradezco mucho haber crecido con ella, será una enorme profesional de quien ya estoy muy orgullosa.

A mi abuelita Rosa, mi segunda mamá, quien sin importar lo que he decidido hasta el día de hoy, siempre ha estado a mi lado. Junto a mi abuelito Rubén, nunca dudaron que lograría todo lo que me propusiera.

Gracias a mis abuelos Juanita y Camilo, por el apoyo brindado y su contante preocupación.

A mi prima Macarena, quien ha sido una parte fundamental desde que crecimos y compartimos juntas. A Macarena le agradezco por siempre hacerme sentir como su hermana. Y a mi madrina Lorena, por el infinito amor, alegría y preocupación que ha tenido conmigo desde que nací.

A mi padrino Rodrigo, por alentarme a entrar a la FCFM.

A mi pareja Matías, mi compañero en la vida, una de las personas más importantes que he conocido. Agradezco su tremenda paciencia y apoyo incondicional. Gracias por hacerme partícipe de su vida y por la alegría, cariño y optimismo que día a día me contagia. Estoy segura que su esfuerzo e inteligencia lo convertirán en un excelente profesional.

A mi amiga Katherine, por todo lo que hemos pasado. Gracias por formar parte de mi vida, por haber aprendido juntas y por la sincera amistad, alegrías y llantos que hemos vivido desde que nos conocimos.

A mis amigos y compañeros de universidad, Bryan y José, por cada uno de los momentos que pasamos juntos y por estar conmigo en los momentos buenos y, sobre todo, en los no tan buenos. Gracias por la amistad incondicional que tenemos.

A mi profesora co-guía y colega Paulina, a quien le debo gran parte de lo que he crecido como persona y profesional, de quien nunca he dejado ni espero dejar de aprender. Sin duda una de las personas que más agradezco haber conocido en este proceso. Gracias por toda la confianza que ha depositado en mí, por todo lo que me ha enseñado y por su preocupación constante.

A Koen Langie, Consuelo Glaría y Williams Calderón, quienes hicieron posible que este trabajo de título pudiera concretarse. Agradezco enormemente toda la ayuda y aprendizaje que me proporcionaron.

Y gracias a todos aquellos que estuvieron conmigo, de una u otra forma, en el transcurso de mi crecimiento y formación profesional.

Table of Contents

Table Index

Figure Index

1. INTRODUCTION: THE ENERGY SYSTEM'S EFFECT ON THE ENVIRONMENT

A Greenhouse Gas (GHG) is any gaseous compound in the atmosphere, which is capable to absorb infrared radiation, catching and holding heat in the atmosphere. By increasing the heat in the atmosphere, GHGs generate the greenhouse effect, which ultimately conduce to rising global temperatures. So then, the global warming would be the climate change phenomenon that needs to be stopped.

With the intention to face the climate change, GHG massive emissions have stimulated the reformulation of energy sources utilized by important GHG contributor sectors like Buildings, Transport, District Heat, Power and Industry. Scaling up to world scenario, global energy sources reformulation would mean the world energy matrix change. This world power matrix represents the total primary energy utilized in the planet, indicating the relative incidence of the sources from which every type of energy comes from. Analyzing Figure 1, among the different energy sources, oil, natural gas and coal take 85.2% of the global matrix. Being fossil fuels the major energy suppliers, it is necessary modify the matrix, adding sustainable energy sources to control the global temperature's increase.

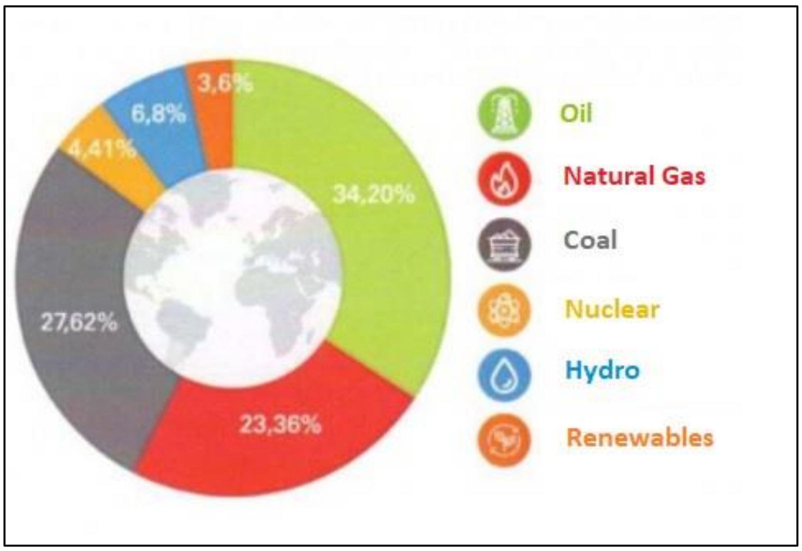

Figure 1: World Primary Energy Matrix. (Bravo, 2018). (BP, 2018).

To regulate this climate change cause, the 2015 Paris Agreement, ratified by 148 nations, defined the main strategy. The plan aims to limit the rise in average annual global temperature below 2°C, regarding to the preindustrial levels. To meet this target, it is necessary the use of renewable energy as well as energy efficiency to reduce GHG emissions across all global sectors. With the help of both, 90% of the total reduction could be achieved in energy-related CO_2 emissions (IRENA, 2018). The GHG reduction success can depend on Hydrogen (H2), which has the potential to be the "missing link" in the energy transition from fossil fuels to renewable low carbon-based systems. From here, H2 is preferably studied as Renewable H2. This Renewable H2 is referred to H2 produced by water electrolysis using renewable energy sources.

1.1. Objectives

- General Objective:
  - Study the development of the existing global H2 market and carry out a technical and economic prefeasibility evaluation of the PEM fuel cell use, fueled with H2 in mobility application at Chilean mining industry.

- Specific Objectives:
  - Describe H2 and study its international development. Specifically, study H2 in terms of existing production methods, number of Hydrogen refueling stations in existence, technologies using H2 and current fuel cell manufacturers.
  - Analyze operating parameters of the available fuel cell technologies in international market and define the advantages of choosing PEM fuel cell for the prefeasibility evaluation.
  - Characterize energy consumption, GHG emissions and the mobility market in Chilean copper mining sector to identify key information for technical and economic evaluation.
  - Carry out the technical and economic prefeasibility evaluation of the PEM technology fueled with H2 and retrofitted to a high tonnage extraction truck (CAEX), used in open pit mining, to compare it with the current technology evaluation. The current conventional technology is referred to the same CAEX operating in Diesel internal combustion engine.
  - Conclude on the viability of the adapted technology in Chile.

1.2. Scopes

The Komatsu 930E-4 is the model truck used to evaluate the CAEX retrofitting with PEM fuel cell fueled with H2.

Within Chilean copper mining, the mobility sector is studied considering the following vehicles of interest:

- Low Profile Trucks / Loaders
- Explosive Trucks
- Off-Highway Trucks

- Light Trucks
- Utility Trucks
- Front Loaders

To characterize Chilean copper mining mobility, the following truck brands are considered: Komatsu, Caterpillar, Liebherr, Hyundai, Atlas Copco, Le Tourneau and Terex.

The prefeasibility study of CAEX retrofitting is evaluated to introduce H2 and fuel cell technology in electric power train CAEXs, which have operations in open-pit mining.

For the prefeasibility study, the truck power calculated and projected through the total travelling time does not consider the acceleration influence in flat roads. Moreover, truck power is considered as a constant value for each route or road division to simplify Lithium-Ion Battery and PEMFC models selection.

In the present thesis work purchase and fuel consumption costs are considered as ownership and operation costs, respectively. Maintenance costs and rent time are estimated according to operations and extractive processes frequency carried out by the haul trucks present in the selected mine.

Only theoretical and statistical conclusions are presented to determine the electric CAEXs retrofitting viability in Chilean open-pit mining.

2. THE SOLUTION: THE H2 AS AN ENERGY VECTOR AND ITS DEVELOPMENT IN GLOBAL MARKET

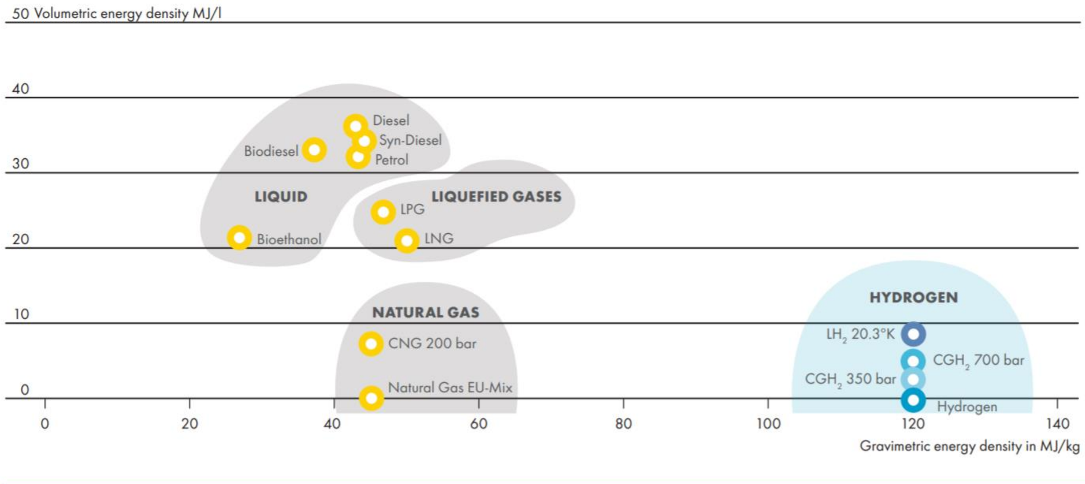

Figure 2: Gravimetric and volumetric energy densities of H2, energy carries and other fuels. (Shell, 2017).

Compared with all the known elements, H2 is the most abundant and lightest. It is odorless and nontoxic. As it can be seen in Figure 2, H2 has the highest energy content per kg. H2 atoms can be separated from water, from hydrocarbons (in coal, petroleum and natural gas) and from biomass. To produce H2, the two most common methods are steam-methane reforming and water electrolysis. The electrolysis or “water splitting” is one of the methods used to produce Renewable H2.

The water electrolysis process, represented in Figure 3, occurs inside an electrolyzer. The electrolyzer is an electrochemical device, which use electricity to separate water into Oxygen (O_2) and H2. The H2 produced, as an energy flexible carrier, can be transported or stored. It can be used for renewable energy storage, allowing renewable H2 conversion into electricity in a fuel cell device. Enabling the possibility of transforming back the electricity into H2 in an electrolyzer.

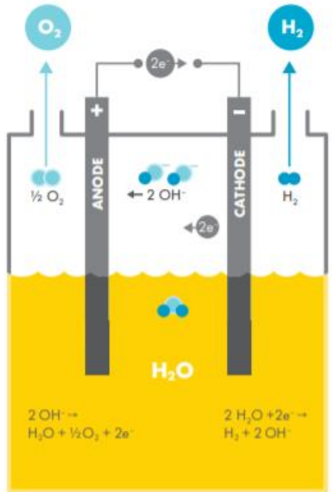

Figure 3: Representation of the electrolysis principle. (Shell, 2017).

H2 is also well known as an energy vector. The term energy vector refers to H2 as an energy-rich substance, which facilitates the transmission, distribution and storage of energy. These three properties are developed with the intention of using H2 at a distance in time and/or space from the primary production site. In fact, H2 can create new connections between centralized and decentralized supply and demand point, which will potentially enhance the flexibility of the overall energy system. H2 should be viewed as the energy carrier around which considerable infrastructure could be constructed, especially for long-distance transport and export purposes. Allowing H2 can link energy sectors with new energy transmission and distribution (T&D) networks in the future global energy system.

A schematic representation of today's global energy system and a potential future low-carbon energy system are shown in Figure 4. Comparing both energy systems scenarios, the key difference lies in the different energy vectors used to supply transport, buildings and industry. Particularly, these sectors depend on the T&D of electricity, heat and fuels via different energy networks. Today's energy system is heavily dependent on fossil fuels and only few connections exist between T&D systems. On the other hand, in a future energy system, H2 energy vector could play a pivotal role connecting different sectors in a low-carbon energy scenario.

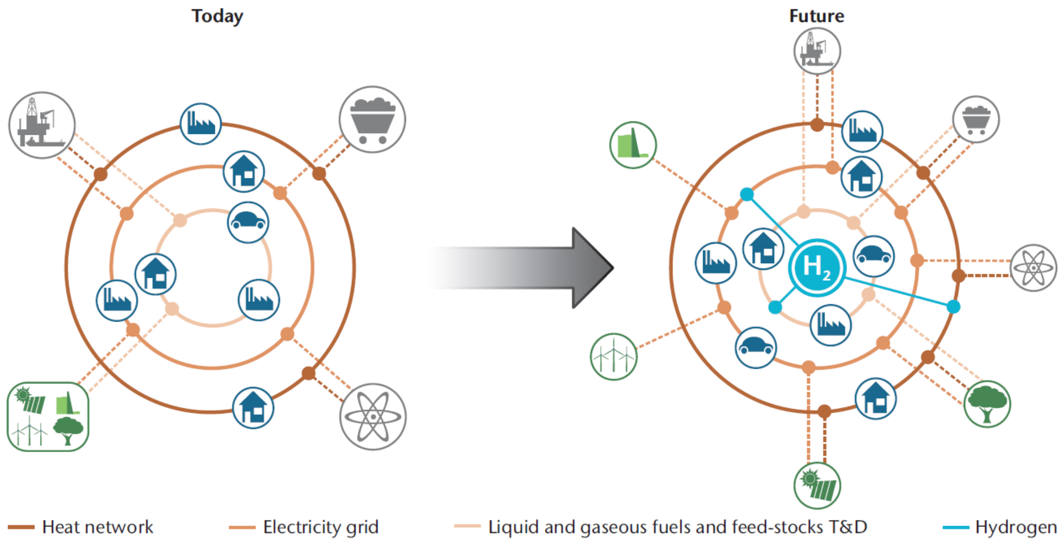

Figure 4: Current and future global energy systems scenarios. (International Energy Agency (IEA), 2015).

Because of its energy vector role, Renewable H2 can feed renewable energy from the power sector into sectors where electrification and decarbonization are difficult to obtain. Moreover, H2 could be the protagonist in Mobility, Buildings and Industry sectors and, at the same time, in the integration of Variable Renewable Energy (VRE). H2 can be injected into the natural gas supply network, adding H2 and blending it with natural gas to defray the cost of building dedicated H2 pipelines. H2 can also be used directly as fuel. Particularly, it is possible to use H2 as fuel to generate electricity inside a fuel cell.

Fuel cells are electrochemical devices in which H2 can be converted back to electricity. Contrasting with batteries, fuel cells operate continuously in the presence of air and H2. Fuel cell technology will gradually start to replace the internal combustion engine for applications like mobility and power generation. In fact, H2 fuel cells are a more viable solution than batteries for applications like heavy duty-transport, non-electrified trains and maritime transport, as H2 technologies allow to store up to 10 times more energy per kg, furthermore it allows for rapid refueling. Despite all these benefits, H2 fuel cell applications have not yet reached an economically competitiveness at present. Reaching competitiveness is interrupted, among others, due to the lack of cost government policies promoting decarbonization, which would enable scale up, activating cost reductions for both H2 production and distribution.

2.1. H2: The Current Market

Now-adays, the H2 industry is well developed. It has decades of operation on several different areas in which H2 is used as a feedstock. The H2 feedstock market has a total estimated value of 115 billion USD. It is expected that this market will grow continuously, reaching a value of 155 billion USD in 2022 (Hydrogen Council, 2018). The H2 feedstock market involves two market segments: centralized-transported H2 production and on site H2 production.

Centralized-transported H2 production refers to H2 generated in a central production facility, which is transported via pipeline, bulk tank or cylinder truck and finally sold to a consumer. While for the on-site H2 production case, the H2 is produced and consumed locally at the point of usage.

The H2 consumption depends on the total H2 global demand. The biggest part of it comes from the chemical sector, specifically for ammonia production and fuels' hydrocracking and desulphurization. The chemical, industrial gas and refining industries use 4,000 TWh of H2 per year, which means 120 million tons of H2 produced each year (IRENA, 2019). Around 48% of the H2 currently produced comes from natural gas, 30% arises as a fraction of the petroleum refining process, 18% is produced from coal and 4% is electrolytic H2 (International Energy Agency (IEA), 2015).

2.2. H2 sources and production methods: past and present

In the late 18th century, the principal H2 production was coal gasification. In coal gasification, H2 is produced reacting coal with steam under high pressure and temperatures to form Synthesis Gas (Syngas). The Syngas consists on a combination of carbon monoxide (CO) and H2. Syngas production can be implemented to produce power, liquid fuels, chemical products and H2 as end-product.

Contrasting with now days, H2 as end-product is produced by oil, coal and natural gas reforming. In fact, natural gas contains methane (CH_4) that can be used to produce H2 with thermal processes. These are steam-methane reformation and partial oxidation. In partial oxidation, the CH_4 and hydrocarbons forming natural gas react with O_2 from air in the oxidation process, producing CO_2 and water. Contrasting with partial oxidation, in steam-methane reforming, CH_4 reacts with steam in presence of a catalyst to produce H2, CO and small amount of CO_2. Using the same fuel, steam-methane reforming is capable to produce more H2 per unit of fuel than is obtained by partial oxidation.

2.3. The rise of electrolysis technology

Since the late 18th century until now, renewable electricity sources have advanced in their development. Among them, wind, solar, biomass, hydro and geothermal are low-carbon sources. In theory also, nuclear energy would be a zero-carbon emission source for H2 production.

This has reinforced the emerging water electrolysis, as a potential zero-carbon process for H2 production. For this process, there are different technologies such as Solid Oxide Electrolyzer (SOEC). In this type of electrolyzer the electrolysis reaction occurs at high temperatures from 500°C to 1000°C. At low temperatures, the reaction occurs in technologies such as Polymer Electrolyte Membrane Electrolyzer (PEMEC) and Alkaline Electrolyzer (AEC).

Both AEC and PEMEC are available from W to MW-scale. In 1927, Nel Hydrogen built the first small AEC installation, testing for pure H2 for fertilizer production at Norsk Hydro at Notodden, Norway (Nel Hydrogen, 2020). Also developed by NEL Hydrogen, a large scale of 400 MW-AEC system is available since April 2017. The system consists on 187 AEC stacks at 450 USD/kW for H2 production (ITP Thermal Pty Limited, 2018).

In 2015, the distributed H2 production cost via electrolysis using off-peak electricity was 3.9 USD/kg H2. For 2020, the distributed H2 production has a cost target of 2.3 USD/kg H2 (Office of Energy Efficiency & Renewable Energy, 2019). According to this cost target estimation, U.S. Department of Energy (DOE) has estimated the H2 threshold cost of 2.0 – 4.0 USD per gal of gasoline equivalent on a cost per mile basis in 2020 (Office of Fuel Cell Technologies, U.S. DOE, 2011).

2.4. H2 use of Fuel Cells: How H2 conversion technology works

Fuel cell is a scalable technology, which is produced in very small to large sizes. Each size of fuel cell can generate only a few W to MW of electricity, respectively. The general fuel cell design and operation, illustrated in Figure 5, consist in two electrodes separated by a solid or liquid electrolyte. This electrolyte carries electrical charged particles between cathode and anode. At the anode, H2 reacts with a catalyst, creating an electron and a positively charge ion. The protons then pass through the electrolyte, while electrons create a current through a circuit connected to the cathode. At the cathode, O_2 reacts with protons and electrons, forming water and heat as fuel cell products.

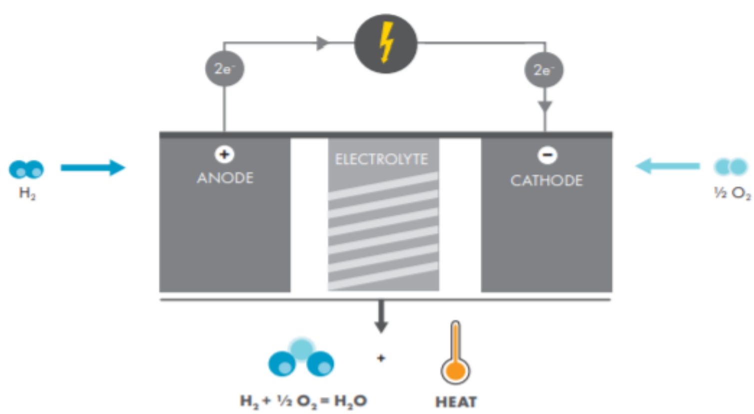

Figure 5: Working principle of the fuel cell. (Shell, 2017).

To produce electric current, fuel cells can be fed with natural gas, liquid fuels such as methanol or Diesel and H2. Particularly, using pure H2 generates as coproduct water vapor. With only water vapor as coproduct, H2 fuel cell has local environmental impact. Despite of this benefit, fuel cells are subjected to a trade-off between power output and efficiency. Fuel cell efficiency is highest at low loads and decreases with increasing power output. In comparison to conventional technologies, fuel cells achieve the highest conversion efficiencies under transient cycles, such as in passenger cars.

Different fuel cells types are represented in Table 1, showing their current performance and design. Into their general design, fuel cells are mainly distinguished by their membrane type and operating temperature.

Table 1: Current performance of key H2 conversion devices. (International Energy Agency (IEA), 2015).

Technology	Electrolyte	Operating temperature [°C]	Power or capacity	Efficiency (HHV)	Initial investment cost [USD/kW]	Lifetim e [hours]	Maturity
Alkaline Fuel Cell (AFC)	Solution of potassium hydroxide in water	23 – 70 or 100 – 250	Up to 250 kW	50%	200 - 700	5,000 – 8,000	Early market
Stationary Proton Exchange Membrane Fuel Cell (PEMFC)	Polymeric membrane	30 – 60	0.5 – 400 kW	32% - 49%	3,000 – 4,000	60,000	Early market
Mobile Proton Exchange Membrane Fuel Cell (PEMFC)	Polymeric membrane	80 – 100	80 – 100 kW	Up to 60%	500	< 5,000	Early market
Solid Oxide Fuel Cell (SOFC)	Solid non-porous ceramic compound	500 – 1,000	Up to 200 kW	50% - 70%	3,000 – 4,000	Up to 90,000	Demonstration
Phosphoric Acid Fuel Cell (PAFC)	Liquid phosphoric acid in a bonded teflon-silicon carbide matrix	150 – 200	Up to 11 MW	30% - 40%	4,000 – 5,000	30,000 – 60,000	Mature
Molten Carbonate Fuel Cell (MCFC)	Molten carbonate salt mixture in a porous ceramic lithium-aluminum oxide matrix	> 650	kW to several MW	More than 60%	4,000 – 6,000	20,000 – 30,000	Early market

3. Global Market: A brief fuel cell stakeholders' rundown

Currently, fuel cells technologies available on the global market include PEMFC, SOFC, AFC, PAFC and MCFC. For these fuel cells, there are manufacturers and integrators investing on them.

The fuel cell integrators are General Electric, General Motors, Hyundai, Honda, Johnson, Matthey, Panasonic, Siemens, Samsung, LG, Sharp, Toshiba and Toyota. Fuel cell integrators depend on fuel cell manufacturers. The highest fuel cell manufacturers are Bloom Energy, Doosan, FuelCell Energy and Plug Power. These manufacturers have built large stationary fuel cells and transportation powering applications using SOFC, PAFC, MCFC and PEMFC technologies, respectively. Particularly, PEMFC technologies developed by Plug Power are being impulse for mobility.

These mobility applications include forklifts, trucks and personal vehicles. For these applications, Plug Power's PEMFC runs on H2, working more efficiently than Bloom's and FuelCell Energy's equipment running on natural gas. Complementing these applications, the DOE has impulse worldwide and specially in California the creation of fuel cell solutions. These solutions consider the construction of large stationary fuel cell installations, the fuel cell integration in micro grids and fuel cell application for grid resiliency. The success of these solutions is reflected on the fuel cells shipments.

Globally the fuel cells shipments grew from 300 MW in 2015 to 500 MW in 2016 and 670 MW in 2017. This evolution explains an annual stationary and transportation fuel cell market growth of 18% to reach more than 2.1 billion USD by 2019. From 2023, it is expected an annual fuel cell market growth rate of 28% (Wesoff, © Greentech Media, 2019).

3.1. Market growth promoted by the power generation demand

As it is represented in Figure 6, the growing demand for power generation is expected to promote the fuel cell market growth. The global fuel cell market is expected to grow from 3,882 million USD in 2017 to 14,918 million USD by 2026. This increase occurs at a Compound Annual Growth Rate (CAGR) of 16.58% between 2018 and 2026 (Market Report Center, 2016).

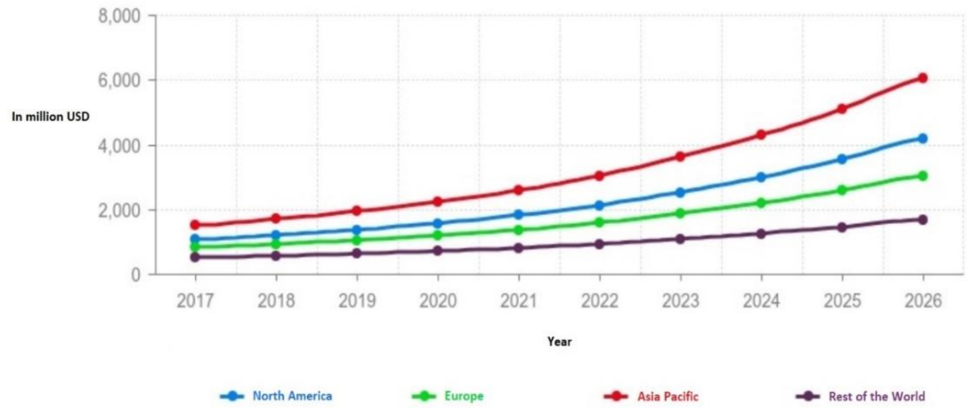

Figure 6: Projected growth of global fuel cell market for each region of the world. (INKWOOD Research , 2019).

The fuel cell market is expected to grow due to the increased electrification of mobility and stationary applications. As such the fuel cell demand is projected to grow with the increasing population in mostly urban areas. The global population is predicted to reach 9.2 billion by 2040 (Exxon Mobil Corporation, 2019), with an ongoing urbanization trend from 52% to 62%, between 2011 and 2035 (Zohuri, 2016).

3.2. Key Performance Indicators (KPI) of the PEMFC Market

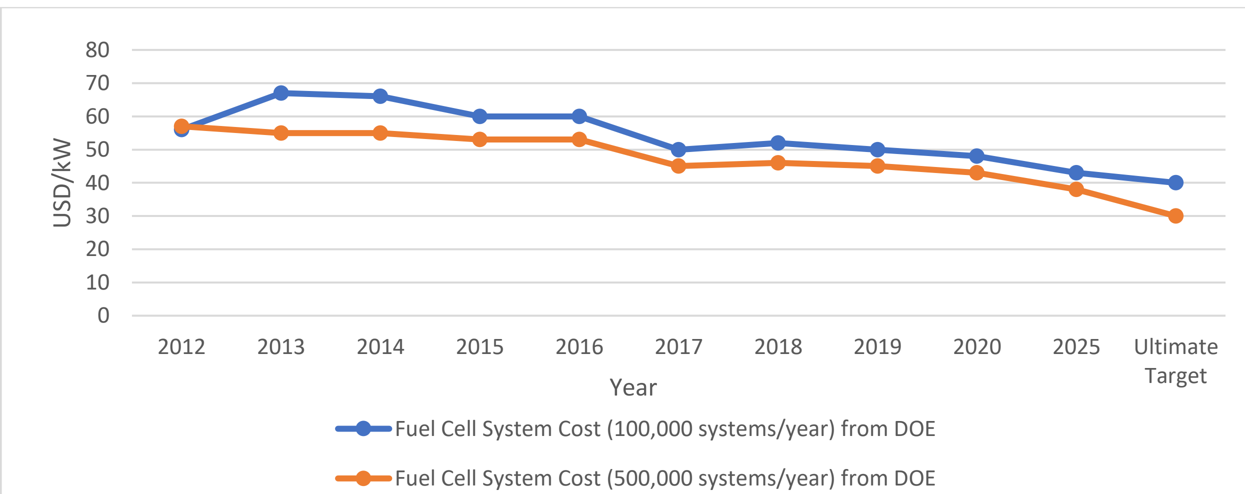

Figure 7: Modeled Capital Cost of a PEMFC System over time projected to different manufacturing volumes. (U.S. Department of Energy, 2017), (U.S. Department of Energy , 2018).

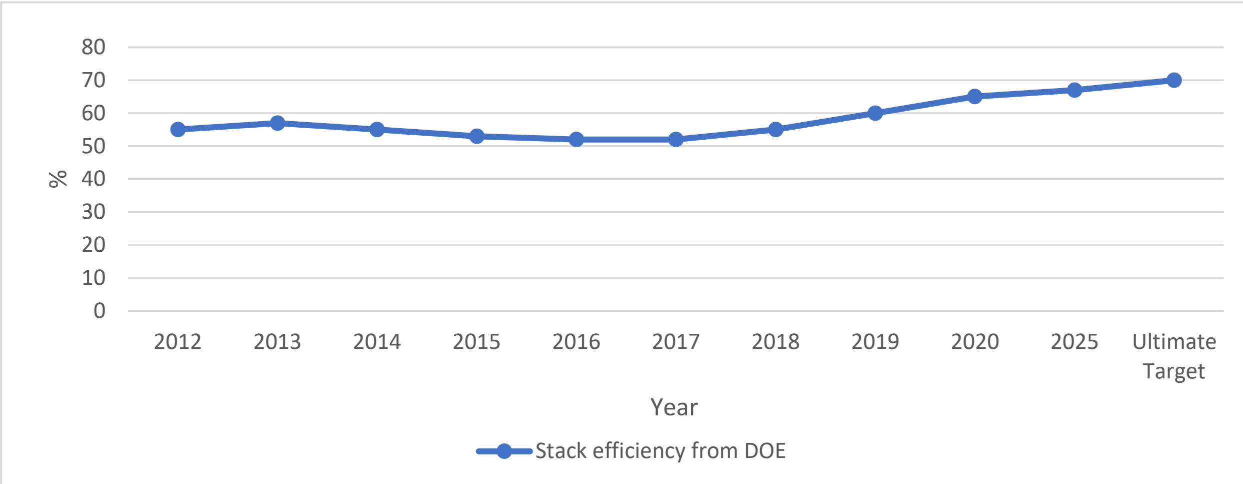

Figure 8: Modeled Efficiency of the PEMFC Stack over Time. (U.S. Department of Energy, 2017).

Analyzing Figure 7, a significant drop in projected system cost takes place between 2016 and 2017. This cost reduction occurs because of technology advances and analysis changes. These factors are related with improvements in performance using advanced cathode catalyst. This improvement along with PEMFC design optimizations have enabled, from 2017 until now, an increase in stack efficiency represented in Figure 8. Also, the scale up of the demand will allow for increased automation of the production process, accelerating the further decrease of costs.

With a projected stack efficiency of 65% in 2020, the projected cost for 2020 does not meet DOE Target. However, the 2020 DOE Target of 40 USD/kW results to be close of 2020 projected cost (U.S. Department of Energy , 2018).

3.3. Production capacity and performance of market players

In Table 2 are represented the main manufacturers involved into the fuel cell market. These actors are classified by fuel cell technology, electrical efficiency, annual production capacity and applications developed. From fuel cell manufacturers studied, the most important are Ballard Power, Plug Power, Hydrogenics, Toyota Boshoku, PowerCell Sweden, Nuvera Fuel Cell and Nedstack. These companies are stakeholders of interest because they develop PEMFC technology for mobility. In their mobility applications, each of them has a large annual capacity of more than 100 MW/year.

Table 2: Stakeholders participating into the Fuel Cell Market.

Manufacturer	Technology	Products	Electrical Efficiency (LHV)	Annual Capacity	Applications
Bloom Energy (Bloom Energy Corporation, 2018) (Wesoff, © Greentech Media, 2019)	SOFC power generators.	From 100 kW to 250 kW fuel cell systems.	50%.	About 1,054 units of 100-kW fuel cells (105 MW/year).	Distributed power generation. Heavy-duty industry (mobility).
Posco Energy (Posco Energy Company, 2019) (Posco Energy, 2015) (Posco Energy, 2018)	MCFC and SOFC.	100 kW, 300 kW and 2.5 MW fuel cell systems.	50% (100 kW and 300 kW systems). 44-49% (2.5 MW system).	100 MW/year.	Stationary systems (MCFC). Building (SOFC).
Doosan Fuel Cell America (Doosan Fuel Cell America , 2017) (Doosan Corporation, 2019)	PEMFC, PAFC and MCFC.	440-460 kW fuel cell systems and PEMFC small system for houses.	43% (440-460 kW systems). 60% (small system).	144 units of 440-kW fuel cells (63 MW/year).	Combined Heat and Power (CHP) from large-scale plants to residential houses.
FuelCell Energy (FuelCell Energy, Inc., 2019) (FuelCell Energy, Inc., 2018) (GlobeNewswire, 2019)	MCFC systems.	1.4-MW, 2.8-MW and 3.7-MW fuel cell power plants.	47% (1.4 and 2.8 MW plants). 60% (3.7 MW plant).	100 MW/year (Connecticut, USA factory, with a potential annual capacity of 200 MW).	On-site power generation in large installations requiring CHP.
Ballard Power (Ballard, 2019) (Ballard, 2019)	PEMFC stacks.	4.4-19.3 kW PEMFC for forklift. 75 kW to 150 kW PEMFC for buses. 0.3-3.4 kW PEMFC for emergency telecom network. 2.3-11.3 kW PEMFC for supplemental power in telecom network. 1.2-kW PEMFC for residential cogeneration.	47-71% (forklift). 62-71% (for heavy-duty app.). 51-67% (emergency backup power fuel cell). 54-64% (supplemental backup power fuel cell). 54-63% (CHP fuel cell).	10,000 fuel cell stacks per year (200 MW/year).	Mobility and stationary power from light to heavy-duty vehicles. Backup power market. CHP market.
Plug Power (Plug Power, 2018) (Plug Power, 2019)	PEMFC.	30-kW PEMFC system for industrial vehicles.	45%.	10,000 units of 30-kW fuel cells per year (300 MW/year).	Mobility (material handling), remote prime power, residential CHP and telecommunication markets.
Fuji Electric (Richter, 2009) (Fuji Electric Co., Ltd., 2017) (Fuji Electric Co., Ltd., 2019)	PAFC systems and PEMFC (in R&D).	Commercial type of 100-kW PAFC power unit. Improved 50-kW PAFC model.	40% (100 kW PAFC system). 50% (PEMFC in R&D).	5 MW/year.	Power generation and cogeneration systems for building applications.

Manufacturer	Technology	Products	Electrical Efficiency (LHV)	Annual Capacity	Applications
SFC Energy (SFC Energy AG, 2018) (SFC Energy AG, 2019)	Direct Methanol Fuel Cell (DMFC) modular units.	45 W, 110 W and 0.5 kW DMFC power units. 2.5 to 20 kW H2 fuel cell.	40%-45%.	About 4,000 DMFC units per year (145 MW/year).	Back up and emergency power supply solutions for households. Vehicle integration for military users (mobility). Off-grid applications (Portable and stationary app.).
Europe's SOLIDpower (SOLIDpower, 2016) (SOLIDpower, 2017)	SOFC systems.	1-1.5- and 2.5-kW fuel cell generators. 10 kW SOFC system (in development).	60% (1-1.5-kW generator). 50% (2.5 kW generator).	1,500 to 16,000 fuel cell generators per year (22 MW/year).	Micro-CHP generators and CHP systems/stacks.
Hydrogenics (Hydrogenics, 2010) (Hydrogenics, 2016) (Thomas, 2016) (Tröger, 2016)	PEMFC (H2 generators and fuel cells).	From 3 kW to 33 kW PEMFC modules. For Heavy Mobility: From 66 kW to 3MW PEM stacks.	55% (PEMFC modules). 49% (PEMFC systems).	160 MW/year.	Industrial processes and fueling stations. Mobility (buses, light-medium duty vehicles and forklifts). Power supply, back-up power and stationary applications.
Panasonic (Quick, 2019) (Panasonic Corporation & Viessman Group, 2019) (Miyake, 2019) (Panasonic, 2019) (FuelCellsWorks, 2019)	PEMFC.	700 W PEM-based CHP fuel cell. 5-kW H2 PEMFC generators (in development).	About 60% (700 W PEMFC). 57% (5 kW PEMFC generators).	About 26 MW/year.	H2 stations (Stationary applications) and commercial facilities (CHP and Mobility).
Toshiba (Toshiba Energy, 2019) (Hidai, 2018)	DMFC and PEMFC.	700 W DMFC unit (residential app.). 700 W, 3.5 kW, 100 kW and 1 MW (stationary app.). For heavy-duty mobility (by end of 2019): 40 kW PEMFC.	42% (fuel cells for residential app.). 51% (fuel cells for stationary app.). 45%-50% (40kW PEMFC).	10 MW/year.	Mobility, stationary and residential applications.
Toyota Boshoku (U.S. Department of Energy, 2016) (Tajitsu & Shiraki, 2019) (Toyota Boshoku, 2019) (FuellCellsWorks, 2019)	Modified PEMFC.	110 kW to 114.6 kW PEMFC stacks (Toyota Mirai Stack). 100-kW solid PEMFC generator.	From 61% to 66% (110-114.6 kW PEMFC). 50% (100-kW PEMFC).	By 2018: 3,000 PEMFC stacks sold (About 330 MW/year). By 2019: About 500 - 1,000 PEMFC stacks sold per month (more than 600 MW/year).	Mobility.
PowerCell Sweden AB (Bodén A. D., 2015) (Bodén A. , 2016) (Ekdunge, 2017)	PEMFC stack and systems.	1-5 kW- and 5-35 kW- based PEMFC stacks. 20-100 kW based PEMFC (in development).	From 40% to 55%.	900MW/year (an increase of more than 22% from 2018 capacity: 800MW/year)	Mobility and stationary applications. CHP applications (telecommunication, power supply to buildings and military).

Manufacturer	Technology	Products	Electrical Efficiency (LHV)	Annual Capacity	Applications
(PowerCell Sweden AB, 2018)					
Ceres Power Holding (Ceres Power Holdings plc , 2019) (CeresPower, 2019)	SOFC systems.	1-5 kW and 10-30 kW SOFC. Low 100-kW PEMFC technologies.	55%-60%.	2 MW/year (with the capacity to expand to 10 MW).	Commercial (stationary uses), mobility and residential markets (CHP). Home systems, data centers and charge points or power stations for electric vehicles.
Nuvera Fuel Cells (Nuvera Fuel Cells, 2006) (Ferraro, et al., 2009) (Nuvera Fuel Cells, 2016)	PEMFC stacks.	10 kW to 150 kW PEMFC engines.	54%.	3,000 PEMFC units per year (200 MW/year).	Mobility, industrial and aerospace applications.
Nedstack (DEMCOPEM-2MW, 2019) (Nedstack, 2019)	PEMFC.	2-10 kW liquid-cooled fuel cell stacks. 1-2 MW PEMFC power plant system. 70-kW PEMFC demonstration power plant.	50% (1-2 MW power plants). 55% (PEMFC stacks and 70-kW power plant).	About 100 MW/year.	Telecom power supply. Grid equipment back up. Mobility and Industrial CHP. Stationary applications.
LG FC Systems Inc. (LG Fuel Cell Systems Inc., 2013) (LG Fuel Cell Systems Inc., 2017) (LG Fuel Cell Systems Inc., 2018)	SOFC stacks and systems.	250-kW SOFC systems.	60%.	140-160 MW/year.	Power supply for local grid. Stationary power applications.

4. H2 REFUELING STATION (HRS) INFRASTRUCTURE

An HRS is a relevant driver for fuel cell applications development. HRSs are service stations designed for vehicle refueling with H2 as fuel. Currently, HRSs are part of fossil fuel refueling stations or can be found as independent stations.

Nowadays, global number of HRSs available to the public is growing. There are 17 new operative HRSs in Germany from 2018, further consolidating Germany as the country with the second largest public HRS infrastructure globally with 60 public stations. Germany is ahead of USA, which has 42 HRSs, and is only surpassed by Japan, which has 96 public HRSs. Compared with the annual growth, in 2018 the number of new HRSs in some locations remains on a steady level, for example in Japan with 9 stations and in California with 6 stations. Summarizing, 48 HRSs were opened worldwide in 2018 (TUV SUD America Inc., 2019). For the next years, there are plans to open new HRSs.

New international plans toward a deployment of additional HRSs are in progress. For 2020, 27 new stations are planned to be operational in the South Korea, 18 in China, 17 in Netherlands, 12 in France and 7 in Canada. The quoted numbers of HRSs correspond only to stations which have at least a designated city (TUV SUD America Inc., 2019). These planned HRSs and the existing ones are designated for passenger cars and for busses and small delivery trucks. Particularly, busses and small delivery trucks are China target and passenger cars are South Korea and Japan target, which can be achieved with HRSs establishment.

Figure 9: Location of worldwide operative HRSs (blue points) and planning HRSs (orange points). (TUV SUD America Inc., 2019).

Represented in Figure 9, there are 152 established and operational HRSs in Europe, 136 in Asia and 78 in North America. On the other hand, Figure 9 also represents 81 HRSs under development. Without counting the 81 HRSs under construction, there are 366 HRSs worldwide. From this number, 273 HRSs are publicly accessible and the others are for dedicated user groups supplying buses or fleet customers. In spite of the HRSs huge worldwide development, there is none of these in Chile. In Chile, the HRSs establishment is not possible yet due to the lack of normative and policies by the government. Because of this absence, fuel cell manufacturers and integrators are not eager to deploy in Chile.

5. APPLICATIONS: H2 TECHNOLOGIES

5.1. Mobility

In mobility, H2 Fuel Cell Electric Vehicles (FCEV) are commercially available for personal use. Medium to heavy-duty FCEV will be available in the next five years as large cars, buses, trucks, vans and forklifts. Into the FCEV market of the next five years, costs are likely to drop with scale, allowing H2 to compete in more segments, such as smaller cars and minibuses.

Particularly, H2 FCEV for personal use segment will perceive a demand increase. By 2030, this growth will induce that 1 of 12 cars sold in California, Germany, Japan and South Korea could be powered by H2 fuel cells. In fact, more than 350,000 H2 fuel cell-based trucks could exist for transporting goods (Hydrogen Council, 2017). Besides, thousands of trains and passenger ships could work without carbon and local emissions.

Promoting zero carbon emissions initiatives beyond 2030, there are plans to use H2 for renewable synthetic fuels creation. This fuels production is intended to decarbonize commercial aviation and freight shipping. Both technologies are harder to decarbonize using just fuel cells fueled with pure H2.

5.2. Feedstock

In feedstock, large amounts of H2 are used in methanol production, refining and ammonia. By 2025, the first refineries and ammonia plants could start producing H2 from clean sources. This Renewable H2 production would enable reducing emissions in petrochemicals and chemicals industries.

In addition to reducing upstream emissions, the carbon capture combined with H2 could be used as industrial feedstock. Feedstock application would allow replacing fossil fuels. Particularly, Renewable Feedstock would depend on carbon capture and H2 production costs. As both costs decrease, up to 5% of methanol and derivatives global production could be based on Renewable Feedstock by 2035 (Hydrogen Council, 2017). For the same year, iron and steel industry is expected to gain momentum. For this industry, it is planned to demonstrate the Renewable H2 use to reduce iron ore to iron by 2030.

5.3. Stationary applications

As the energy system relies increasingly on renewables, H2 could play a growing role in renewable electricity production and storage. By 2030, a surplus renewable electricity of 250 to 300 TWh could be stored as H2 for end-use segments (Hydrogen Council, 2017). From this H2 stored for end-use segments, more than 200 TWh of electrical energy could be generated in large power plants. This electrical generation could be designated to feed from residential houses to huge power plants (Hydrogen Council, 2018). Particularly, fuel cell power plants growth could be impulse by carbon-based power plants replacement. Fuel cell power plants are based on fuel cell stacks generators fueled with H2. For that reason, these power plants are classified as zero-carbon technologies.

CHP applications are planned to be improved as potential zero-carbon technologies, if both heat and electricity are required. CHP applications refers to processes in which, in addition to the generated electricity, the heat produced is also used. The heat produced as a by-product of CHP is used to cover part of the buildings heat demand. The mostly electricity-led mode of operation results in a low thermal output from fuel cell heating systems. Stationary fuel cells are particularly suitable for buildings with a low space heating requirement. Moreover, if stationary fuel cell systems are operated with natural gas as fuel, an existing natural gas infrastructure can be used. Currently, H2 is blended with natural gas into public natural gas networks for CHP stationary applications, for example domestic energy supply illustrated in Figure 10.

For fuel cells over thermal power processes, one of the biggest advantages is the direct electrochemical conversion during electricity and heat generation and the associated higher electrical efficiency. In CHP mode, fuel cells can achieve up to 95% of efficiency. The electrical efficiency is up to 45%. Furthermore, fuel cell CHP systems are characterized by high efficiencies over all load points.

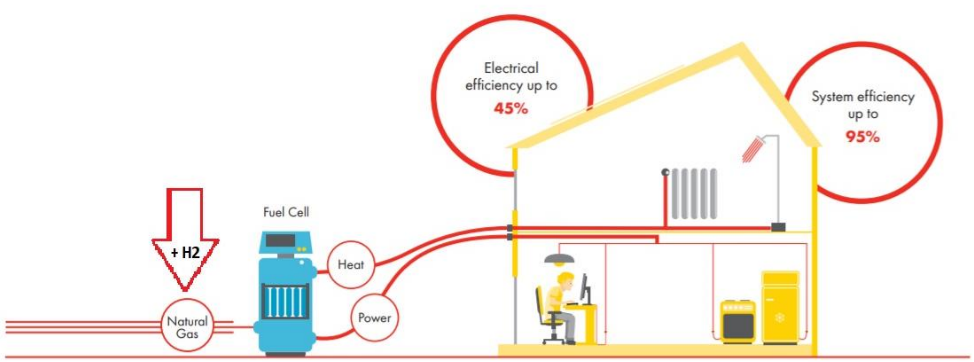

Figure 10: Fuel cell system as a part of domestic energy supply. (Shell, 2017).

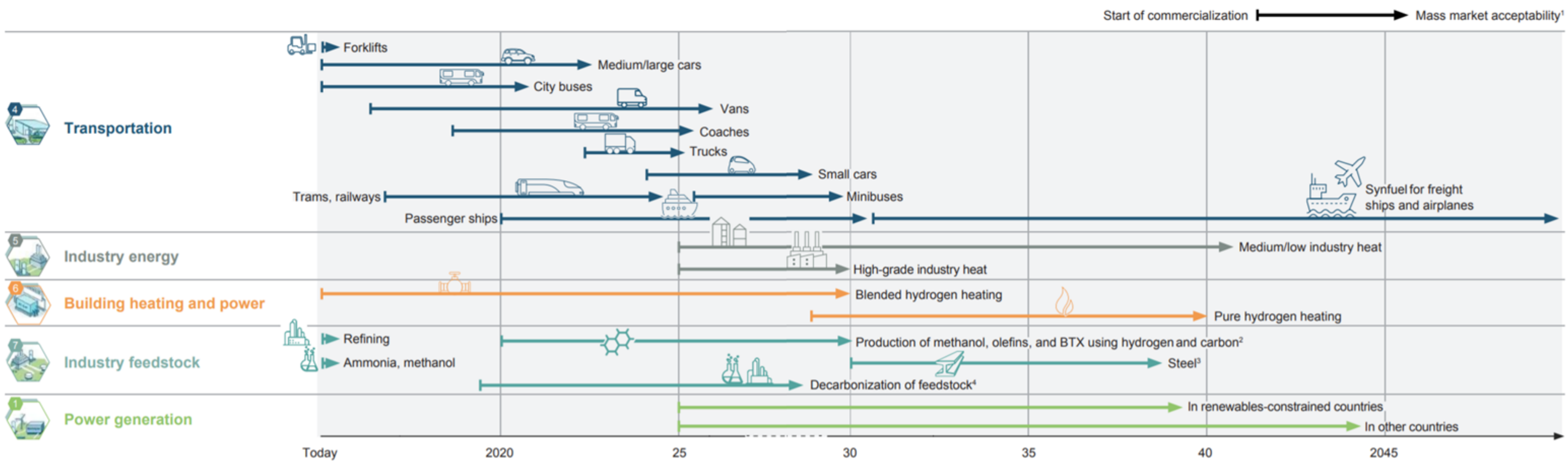

Figure 11: Overview of the H2 technology deployment for the next years (Hydrogen Council, 2017).

6. NATIONAL ENERGY CONSUMPTION IN CHILEAN COPPER MINING SECTOR

Copper production and energy consumption have been historically correlated. From 2001 to 2018, the Chilean copper mining production have remained stable, growing at an average annual rate of 1.3%. At this growing rate, national copper production reached to 5.8 million metric tons (MT) in 2018. For the same period from 2001 to 2018, Chilean mining energy consumption increased at an average annual rate of 4.7%, reaching to 176,745 TJ in 2018 (COCHILCO , 2019).

In 2018, copper mining energy consumption of 176,745 TJ represented a 14% of the country's aggregate consumption. From the 176,745 TJ, electricity consumption achieves 94,153 TJ and fuels consumption 82,592 TJ (COCHILCO , 2019). Figure 12 represents both consumption segments and the copper production from 2001 to 2018.

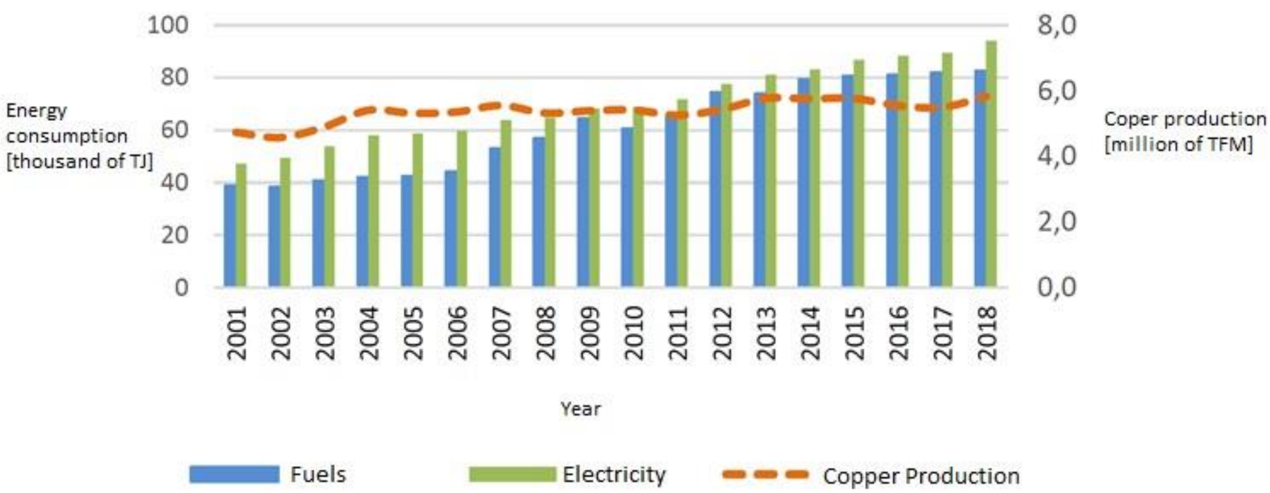

Figure 12: Energy consumption and copper production projected from 2001 to 2018 (COCHILCO , 2019).

6.1. The Copper Mining Energy Consumption's Participation in the National Energy Consumption

Mining sector is one of the main Chilean energy consumers. In fact, mining segment accounts for 14.1% of the country energy consumption. Analyzing Figure 13, this percentage have experimented progressive marginal rises from 2006 to 2017. Among the same years, electricity consumption has remained relatively stable around 33% of the national electricity consumption. In the same period, Diesel consumption has increased its participation from 11.5% to 19.4% of the national Diesel consumption (COCHILCO , 2019).

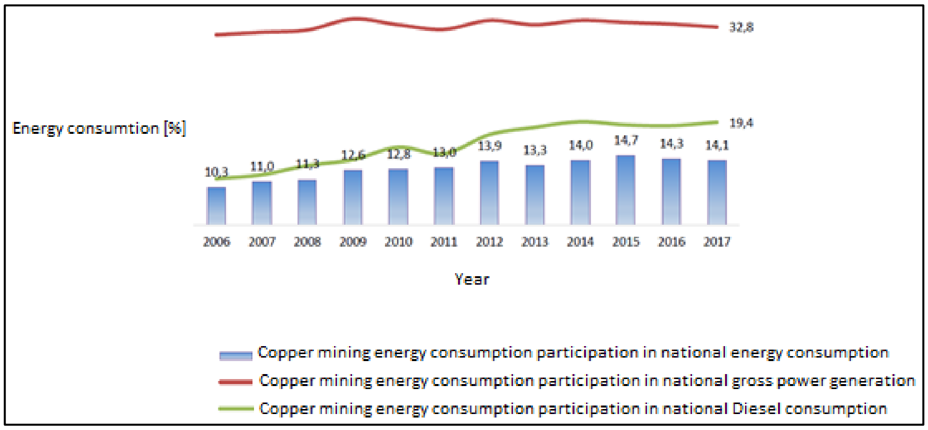

Figure 13: Copper mining energy consumption by sector as percentage of national energy consumption from 2006 to 2017 (COCHILCO , 2019).

6.1.1. Aggregate fuel energy consumption

Figure 14 shows fuel matrix changes implemented in Chilean copper mining industry. From the most important changes, Diesel has gained participation as mining operations grow. Diesel participation in fuel matrix changes from 62.7% in 2001 to 90.4% in 2018. On the other hand, Enap 6 participation in fuel matrix changes from 27.9% in 2001 to 4.4% in 2018. Decrease in Enap 6 use responds to air environmental regulations, controlling emissions and visible gasses in refining ovens. Replacement of Enap 6 with natural gas and conventional burners substitution for a more efficient ones were some of the most relevant environmental actions (COCHILCO , 2019).

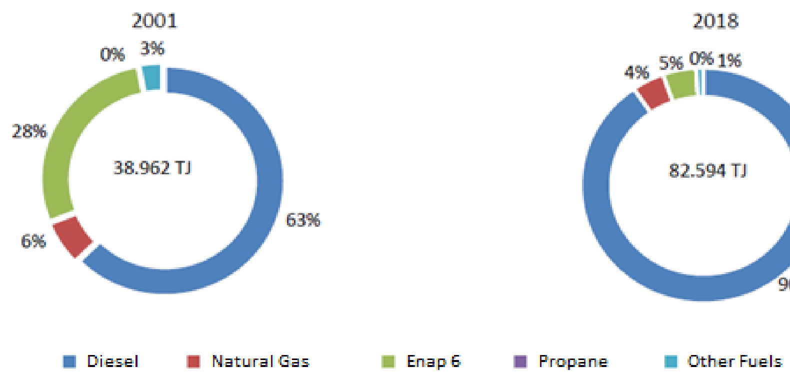

Figure 14: 2001 and 2018 fuels participation in Chilean Copper mining fuel consumption (COCHILCO , 2019).

6.2. GHG national situation

Among GHG controlled, emissions are composed by CO_2 (78.7%), CH_4 (12.5%), N_2O (6.0%) and fluorinated gases (2.8%) (Alta Ley Corporation, 2019). GHG emissions are measured by type, which are classified as scope 1, scope 2 and scope 3 emissions. Scope 1 emissions are direct GHG emissions from owned or controlled sources and operations. Scope 2 emissions are indirect emissions from the generation of purchased energy. Scope 3 emissions are all other indirect emissions (not include in scope 2) that occur in the value chain of the reporting entity, including emissions upstream and downstream.

According to the last public biennial report for climate change update in Chile, 2016 country GHG emissions reported were 111,677,500 ton of CO2 eq. (Ministry of Environment, Government of Chile, 2018). The GHG emissions reported consider 4 sectors: Industrial Processes and Products Use (IPPU), Agriculture, Residues and Energy. As it is illustrated in Figure 15 (Left), Energy sector represents 78% of the country's total GHG emissions, which means 86,133,900 ton of CO2 eq. emitted by the Energy sector (Ministry of Environment, Government of Chile, 2018). Also represented in Figure 15 (Right), Energy sector integrates 4 subsectors of which Manufacturing Industry and Coal represents 19% of the total GHG emissions in Energy. Considering only scope 1 emissions, this percentage denotes 16,129,200 ton of CO2 eq. emitted by Manufacturing Industry and Coal sector (Ministry of Environment, Government of Chile, 2018).

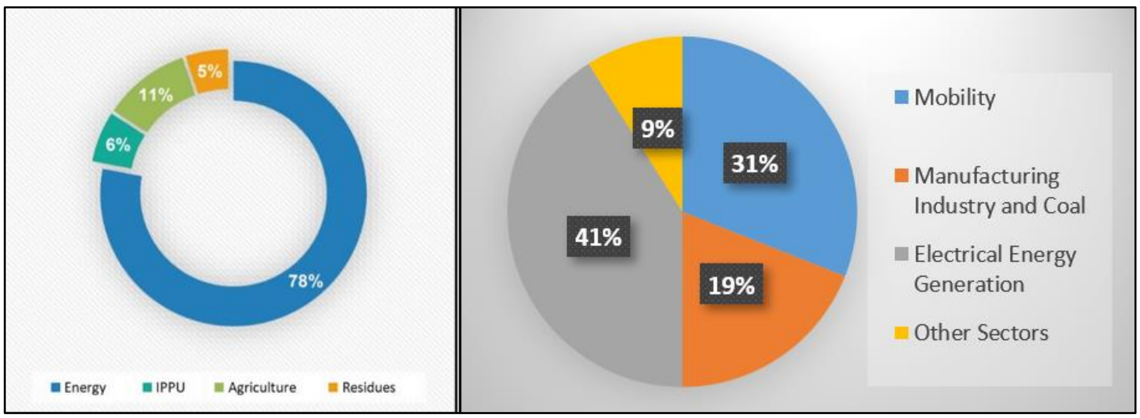

Figure 15: (Left) GHG emissions participation per national sector. (Right) GHG emission participation per subsector in Energy industry. (Alta Ley Corporation, 2019).

At the same time, Manufacturing Industry and Coal sector integrates other subsectors. Illustrated in Figure 16, the biggest contributor subsector to the Manufacturing Industry and Coal sector's GHG emissions is Mining Industry. Specifically, Mining Industry registered 7,966,800 ton of CO2 eq. in scope 1 emissions (Ministry of Environment, Government of Chile, 2018) and 15,281,000 ton of CO2 eq. in scope 2 emissions. Considering only scope 1 and scope 2 emissions, Mining Industry reached 23,248,000 ton of CO2 eq., representing 21% of the total country GHG emissions (Ministry of Environment, Government of Chile, 2019).

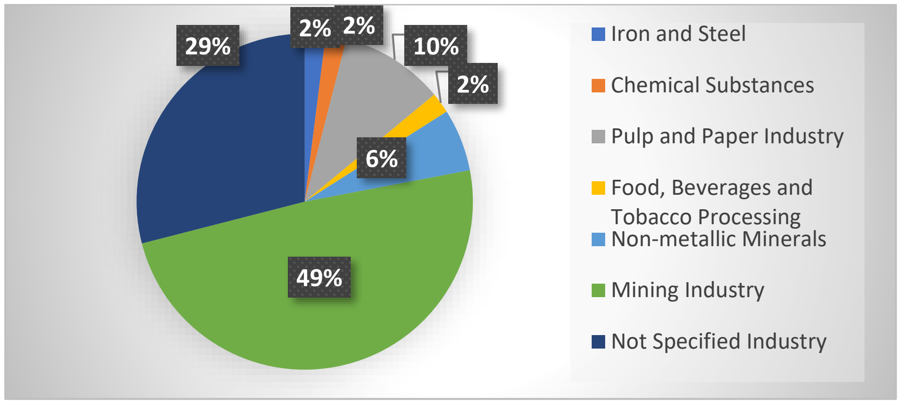

Figure 16: Participation of each Manufacturing Industry and Coal subsector in total GHG emissions of the sector (Alta Ley Corporation, 2019).

6.2.1. GHG emissions in Chilean Copper mining sector

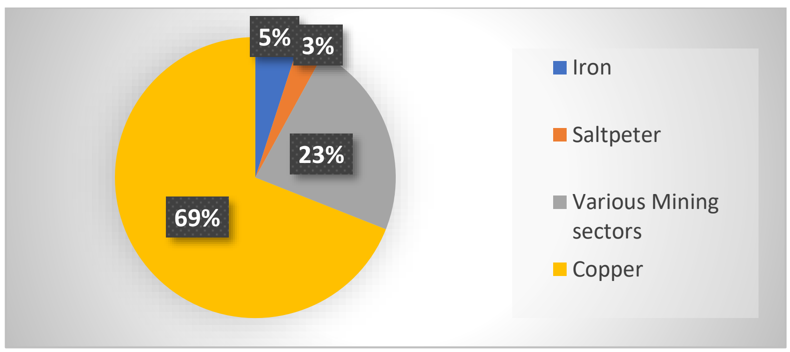

Figure 17: Participation of each Mining Industry subsector in total GHG emissions of the sector (Alta Ley Corporation, 2019).

Among all Mining Industry subsectors, Copper business achieves 69% of the total GHG emissions in Mining Industry Figure 17. In Figure 18, 2018 scope 1, scope 2 and scope 3 emissions in Copper Industry registered 5.6%, 12.8% and 5.2% of the total country GHG emissions, respectively. In 2019, the scenario was similar with 5.5% (scope 1), 13.1% (scope 2) and 5.3% (scope 3) of the country GHG emissions. Both 2018 and 2019 country emissions scenarios are presented considering total country GHG emissions of 109 and 108 million ton of CO2 eq., respectively (Climate Action Tracker, 2020).

In 2018 copper industry direct emissions Diesel was the principal emission source, achieving 90% of the total copper mining scope 1 emissions. In 2019, Diesel continued being the main responsible of the copper industry direct emissions, contributing with 90.4% of the total scope 1 emissions (COCHILCO , 2019) (Alta Ley Corporation, 2019) (Ministry of Environment, Government of Chile, 2018). From 2010 to 2019, Figure 18 represents increases of 36%, 31.5% and 33% in annual copper mining scope 1, scope 2 and scope 3 emissions, respectively. Particularly, scope 1 emissions growth is due to raises in copper concentrate production and in distances from extraction site to processing plant (Alta Ley Corporation, 2019).

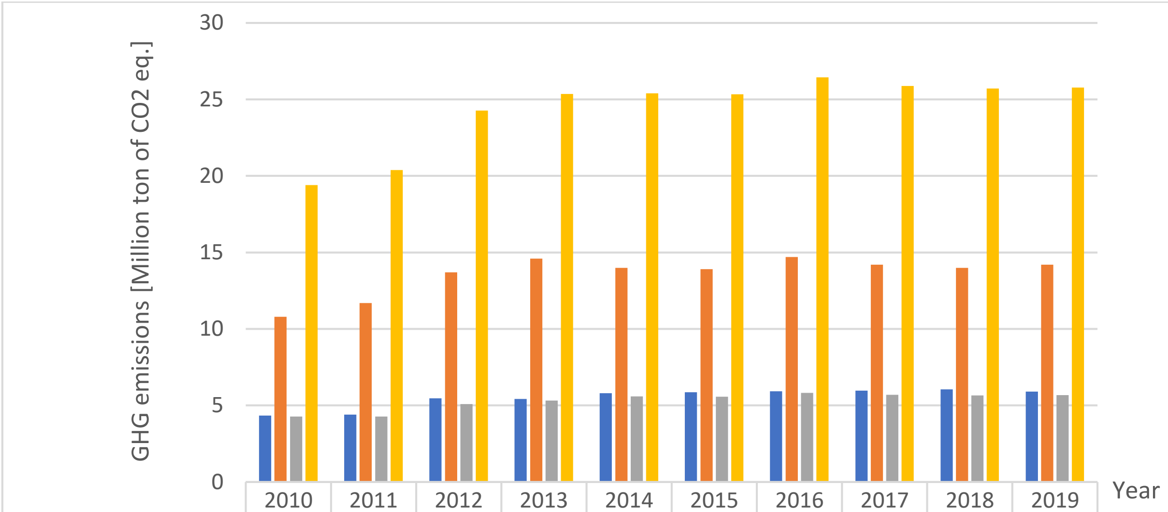

Year	2010	2011	2012	2013	2014	2015	2016	2017	2018	2019
Scope 1 emissions	4,34	4,4	5,47	5,43	5,81	5,86	5,92	5,98	6,06	5,9
Scope 2 emissions	10,8	11,7	13,7	14,6	14	13,9	14,7	14,2	14	14,2
Scope 3 emissions	4,3	4,3	5,1	5,3	5,6	5,6	5,8	5,7	5,7	5,7
Total emissions	19,4	20,4	24,3	25,4	25,4	25,3	26,4	25,9	25,7	25,8

Figure 18: Annual GHG emissions, rated by type, in Chilean Copper mining sector (Own creation). (Alta Ley Corporation, 2019) (COCHILCO, 2019) (Chile Foundation, 2018) (COLLAHUASI, 2019) (COCHILCO, 2017) (COCHILCO, 2016) (Ministry of Environment, Government of Chile , 2011).

7. STUDY OF MINING TRUCKS

Diesel is a significant energy source for the mining industry. Diesel is used for material transport processes such as the hauling of ore and overburden. Specifically, one of the key Diesel-using activities comes from mining trucks. In fact, a typical high tonnage truck in open-pit mining operations consumes 3,600 l of Diesel per day (CORFO Government of Chile , 2017), which means 1,314,000 l of Diesel consumed per year for each open-pit heavy duty truck.

Globally, in surface mines, trucks are used to haul overburden and ore from the pit to a dump site, stockpile or to the next stage of a mining process. Haul trucks are used in combination with other equipment such as excavators, loaders and diggers, according to the site layout and production capacity.

In Chile, mining trucks are deeply involved in uses as Low-Profile Loaders, Front-End Loaders, Low Profile Trucks, Off-Highway Trucks, Utility Trucks, Light Trucks and Explosives Trucks.

Considering trucks utilized for the main purposes mentioned, the number of Chilean mining trucks operative in 2019 were 2,521 (COCHILCO, 2019) (COCHILCO, 2017) (COCHILCO, 2016) (COCHILCO, 2015) (Thompson Reuters, 2015). The total number of mining trucks mostly considers brands positioned with greater presence in large-scale mining in Chile. Caterpillar, Komatsu, Liebherr, Atlas Copco, Hyundai and Le Tourneau complete almost the 100% of participation from the 2,521 mining trucks.

7.1. Types of Trucks in Chilean open-pit mines

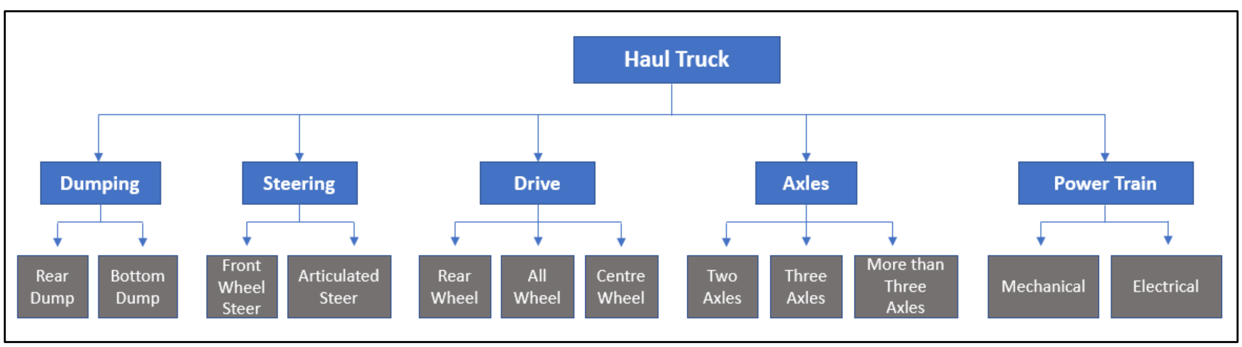

Figure 19: Haul truck types in Chilean open-pit copper mines, with performance and components classification (Own creation). (Soofastaei, Karimpour, Knights, & Kizil, 2017).

Different types of trucks used in open-pit copper mines are shown in Figure 19. There are three main types of trucks: rear, bottom and articulated dump trucks.

In rear dump trucks, the tray is mounted on the truck frame and dumping is carried out by a hydraulic hoist system raising the tray. Rear dump trucks are very flexible units capable of handling all types of material, being the most common haulage truck in Chile.

On the other hand, bottom dump trucks provide faster dump times and higher payload for the same engine horsepower, but at the cost of grade ability and maneuverability. In general, bottom dump trucks are used in strip coal mines where the ramp gradients are kept at 5% or less (Soofastaei, Karimpour, Knights, & Kizil, 2017).

At last, articulated dump trucks tend to be smaller and of lighter construction, being around 50 ton the truck's maximum size. Articulated dump truck main application focusses on wet and poor road conditions.

Considering rear, bottom and articulated dump trucks the mining trucks' classification types in open-pit mines by operation, mining trucks are also catalogued by size classes or by gross power. Table 3 shows mining trucks classification by size classes or payload, with respective gross powers range for each payload range.

Table 3: Payload and gross power range classification for haul trucks working on open-pit mines (The Parker Bay Company, 2020) (Hawthorne Cat, 2014) (PwC – Mining Intelligence and Benchmarking, 2013).

SIZE CLASS [metric ton]	GROSS POWER [hp]
90 – 110	834 – 1200
127 – 150	1290 – 1487
154 – 190	1600 – 2100
218 – 255	2057 – 2701
290	2701 – 3501
308 – 363	2701 – 4023

7.2. Electric and Mechanical power train systems in Haul Trucks

As it was represented in Figure 19, haul trucks are also classified by power train. There are two types of power train systems: mechanical and electric drive haul truck.

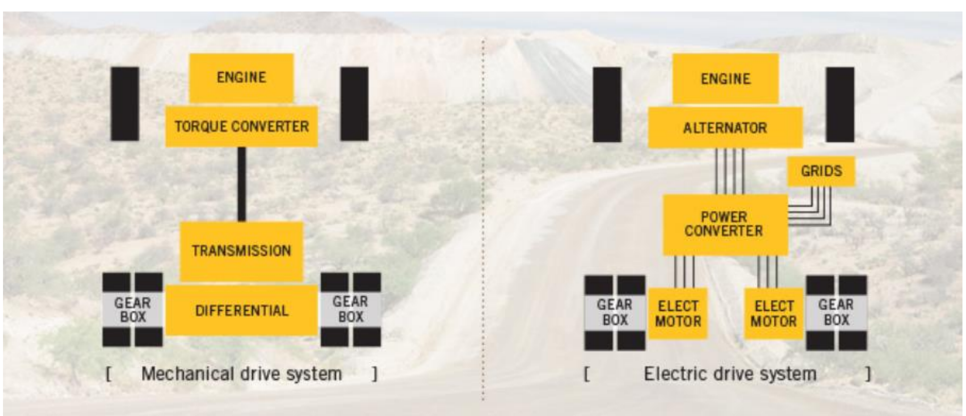

Figure 20: Haul trucks' internal configuration for Mechanical (Left) and Electric (Right) power train (© Caterpillar, 2020).

Being illustrated in Figure 20 (Right), electric drive layout consists of an engine-driven alternator supplying AC current to a DC control box through a rectifier. Then, DC power is taken through an inverter, which provides AC current to the drive motors.

Mechanical drive system showed in Figure 20 (Left) is characterized for being completely automatic, designed to minimized impacts in motor drive line. So, the effects in drive line are controlled by mechanical drive's main components, which are torque converter, gearbox, differential and final drives.

Both power train systems are presented in different mining truck's size classes, which depend on road layout and customer preference specifications. However, there is a usual relation among payload and power train system of haul trucks configuration, which is showed in Table 4. The relation among both parameters is defined considering 180 ton and above-haul truck is more reliable and performs better with electric power train system. For haul trucks payload below 100 ton, the mining industry generally prefers the mechanical power train system, which confers to the truck a more efficient haulage, in terms of production. Between 100- and 180-ton size class, haul truck market seems to be indifferent for both power train configurations, being customers preference and mines specifications decisive in power train preference.

Table 4: Relation between payload size class and power train system of haul trucks in open-pit mines (INACAP, 2020).

PAYLOAD [ton]	POWER TRAIN CONFIGURATION
< 100	Mechanical
100 – 180	Mechanical or Electric
> 180	Electric

8. ELECTRIC DRIVE TRUCKS INVENTORY AND MINING TRUCK RETROFITTING

At 2019 first quarter, from the 2,521 mining trucks available and involved in applications like Low-Profile Loaders, Front-End Loaders, Off-Highway Trucks, Utility Trucks, Light Trucks and Explosive Trucks, there are 1,043 electric drive haul trucks destinated for Chilean open-pit mining (COCHILCO, 2019) (COCHILCO, 2017) (Thompson Reuters, 2015) (MCH Chilean Mining , 2015) (MCH Chilean Mining, 2013). Showing in detail the mining truck brands with their respective models and performance specifications, Table 5 summarizes relevant information about the 1,043 electric haul trucks considered.

Table 5: Number of electric drive systems per haul truck model and brand, with respective power gross specification, in Chilean open-pit mining (COCHILCO, 2019) (COCHILCO, 2017) (Thompson Reuters, 2015) (MCH Chilean Mining , 2015) (MCH Chilean Mining, 2013)

Brand	Model	Gross Power [hp]	Existence	Total
Komatsu	630E	1800 - 2000	16	888
	730E	1860 - 2000	62	
	830E	2500	184	
	930E	2700	569	
	960E	3400	48	
	980E	3500	9	
Liebherr	T282	2780	36	92
	T282B	3500	48	
	T282C	3500 - 3650	8	
Le Tourneau	L-1400	2000	6	31
	L-1800	2000	1	
	L-1850	2000 - 2500	22	
	L-2350	2000	2	
Caterpillar	MT4400 AC	2500	6	23
	CAT 794	3500	4	
	CAT 795	3400	13	
Terex	MT-3700B	2000	3	9
	MT-4400AC	2500	6	
Total Number of Electric Drive Haul Trucks				**1043**

Analyzing Table 5, among all the brands studied, Komatsu leads the electric drive haul trucks market in Chilean open pit mining with 888 units in operation (85%). On the other hand, with its T282 electric truck versions, Liebherr counts with 92 operative units (9%). By last, Le Tourneau, Caterpillar and Terex achieve the 6% of the electric trucks market with 63 active units for open pit mining.

Considering the existences and gross power developed for each electric truck presented in Table 5, the 1,043 electric haul trucks bring 2.083 GW of power capacity. In other words, 2.1 GW of potential capacity to achieve through the haul trucks retrofitting using Hydrogen PEM fuel cell technology, with the intention to decarbonize the open pit mining sector.

To demonstrate the Hydrogen PEMFC use in mining applications, specifically in haul trucks for mobility, it has projected to evaluate the retrofitting of an ultra-heavy-duty mining truck. The model chosen for the evaluation is the Komatsu 930E-4 ultra-class mining truck.

9. ESTIMATION OF THE OWNING AND OPERATING COSTS

Comparing both scenarios, the heavy-duty mining truck retrofitted with H2 PEM fuel cell and the same mining truck available in current market, it has estimated the total cost for each situation through a calculation strategy.

Firstly, to introduce the methodology used, it is important to recognize two types of equipment costs: owning costs and operating costs. Owning costs refer to the costs incurred even if the machine is not working. The owning costs include depreciation, interest, taxes and insurance. On the other hand, operating costs are the costs involved in the machine operation, such as costs for repair, fuel, lubricants, tires, special items and operator's wages.

For the next sections, it has explained one method, which estimates the owning and operating costs of the heavy-duty truck equipment.

9.1. Chilean open pit mine selection

For the technical and economic prefeasibility of the CAEX retrofitted, there has been selected an open pit mine in Chile to evaluate the technology performance with the haul truck operation. The mine chosen is the Spence Open Pit Mine from the BHP Group Ltd. Represented in Figure 21, Spence is a copper mine located 50 km SW from Calama, Chile. At Spence mine, overburden is removed after blasting, using a truck or loader and shovel. Specifically, inside the mine are operated the Komatsu 930E ultra-class mining trucks, which is the model of interest for the evaluation.

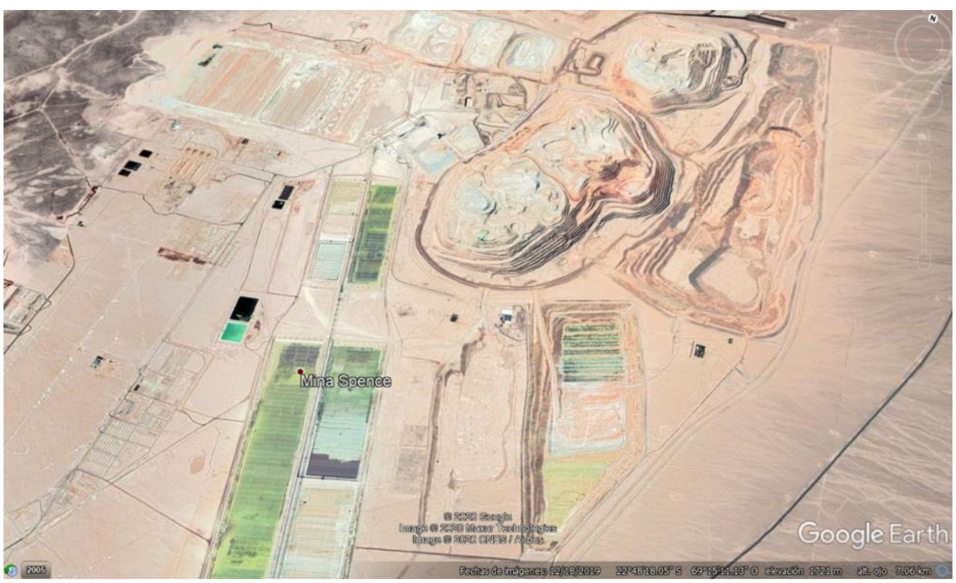

Figure 21: Spence Open Pit Mine in 2019.

To evaluate the Komatsu 930E-4 mining truck performance, a closed path is drawn in Figure 22. Drawn the path in Figure 22, each truck starts at the Crusher with no payload, goes down to the Mining Shovel to be loaded and finally goes back to the starting point, passing through the same path previously traveled, to tip the ore in the Crusher.

Figure 22: Closed circuit path (in white line) travelled by the entire fleet of trucks considered for the evaluation.

Evaluating the potential decarbonization capacity in Chilean copper mining, it is considered that the closed circuit drawn is traveled by a fleet size of 1,043 electric drive trucks. The 1,043 CAEX calculated in Table 5 are the specific sector in mobility which is planned to be retrofitted replacing the Diesel engine by the fuel cell and battery system.

9.2. Truck Trip Methodology for Retrofitted and Conventional Technology

The technical and economic evaluation requires the performance parameters calculation of the retrofitted and the conventional Komatsu 930E-4, which are dependent on road condition and truck weight configuration.

Considering several road conditions at the entire closed-circuit, the path has been divided into eight sections. For each section, road features and truck operational parameters have been measured with Google Earth Application and calculated with a specific method, respectively.

9.2.1. Power Train configurations for Retrofitted and Conventional Technology

The internal configuration of both applications, the conventional and retrofitted Komatsu 930E-4 power trains, are represented in Figure 23 and Figure 24, respectively. For each power train configuration, below each component is designated the power conversion rate.

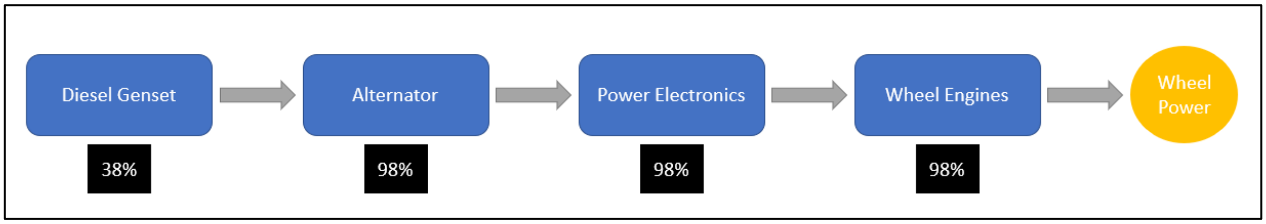

Figure 23: Power train components for a conventional Komatsu 930E-4, with respective efficiency rates of electrical transmission.

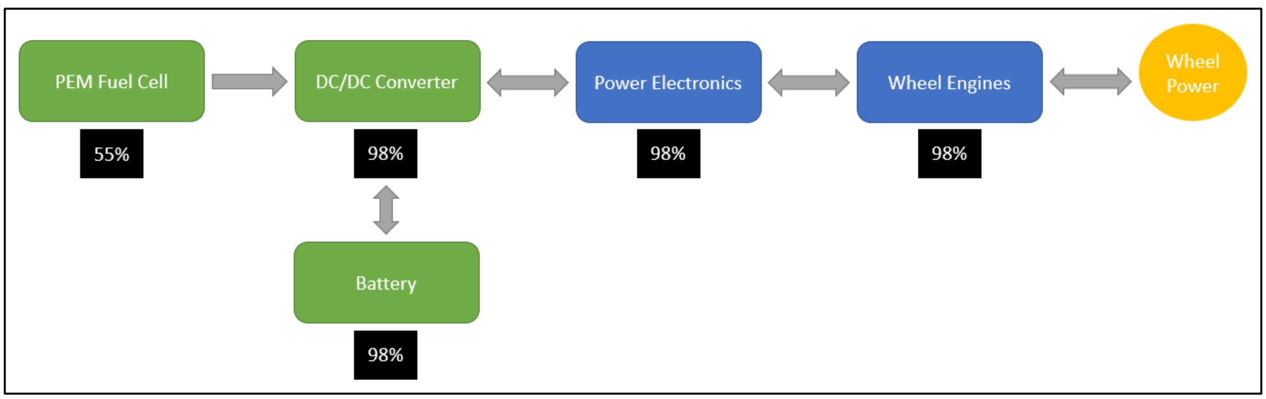

Figure 24: Power train components for Komatsu 930E-4 retrofitting, with respective efficiency rates of electrical conversion.

Analyzing Figure 23, the Diesel Genset is the diesel generator, which connects the diesel engine with the truck alternator. For both conventional and retrofitted truck power trains, the Power Electronics are responsible for converting and controlling electric power in electric truck system. Power Electronics include inverter, converter and on-board charger.

9.2.2. Truck Operational Parameters and Fuel Cost Calculation

Haul truck fuel consumption is a function of various parameters. The key parameters affecting the energy consumption include the payload management, the model of the truck: Komatsu 930E-4, the Grade Resistance (GR) and the Rolling Resistance (RR). The effects of the Gross Vehicle Weight (GVW), the truck speed (v) and the Total Resistance (TR) on the energy consumption of the haul truck have been examined. Represented in Equation 1, TR is the sum of RR and GR when the truck is moving against and down the grade of the road.

$$TR = RR + GR$$

Equation 1: Total Resistance Formula. (Komatsu, 2013) (Komatsu, 2007).

The Rimpull curve defines the maximum operating speeds for different road configurations (GR and RR values). For Komatsu 930E-4, the RR working against the truck is estimated at 2% (for loaded and empty truck). On the other hand, GR is the positive road grade resistance working against the truck when truck is going up. When the truck is going down, GR is a negative percentage, because the grade favors making the truck roll away.

The forces previously mentioned are present in truck movement through the three road configurations considered in the closed-circuit path. For the three configurations, if a truck moves at a constant speed, then there would be a forces balance between TR (forces opposed to the truck movement) and the thrust force, which impulses truck to keep moving.

Particularly, Figure 25 presents a schematic diagram of Komatsu 930E-4 and the key forces affecting truck performance going up.

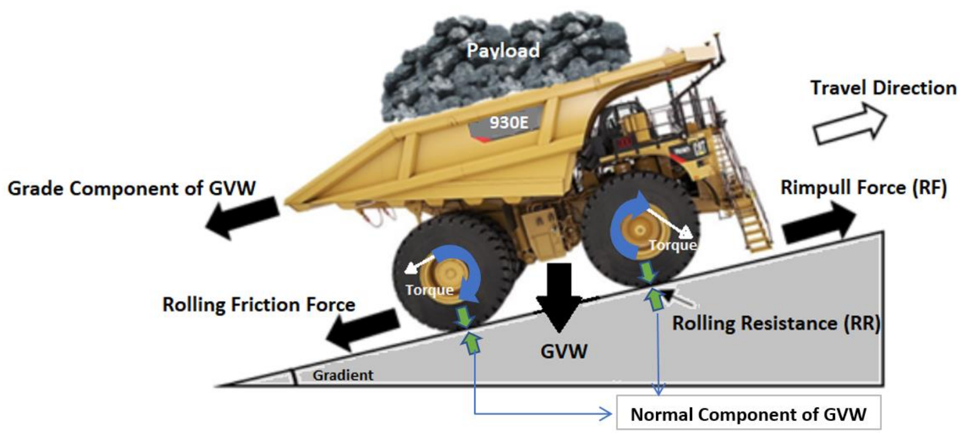

Figure 25: Komatsu 930E-4 schematic forces diagram (Own Creation). (Barrientos, 2018) (Komatsu, 2013) (Komatsu, 2007).

In Figure 25, the Rimpull Force (RF) is the force available between the tyre and the ground to propel the machine. According with Equation 2, RF is related to the truck wheel radius (r) and the Torque (T) that the truck is capable of exerting at the point of contact between its tyres and the ground.

$$RF = \frac{T}{r} = R \cdot g$$

Equation 2: Rimpull Force formula. (Komatsu, 2013).

In Equation 2, g is the gravitational acceleration and R represents the Rimpull (in kg).

To obtain RF and *v*, Rimpull-Speed-Grade curves (or Rimpull Curve) is utilized. The Rimpull Curve, presented in Figure 26, defines the maximum operating speeds for several road configurations (GR and RR). To exemplify, if a loaded Komatsu 930E-4 (320 ton of GVW) travels up with a 12% of TR (Komatsu, 2007), there is one way to read the Rimpull-Speed-Grade curves graph:

I. Finding the intersection between the TR line (12%) and the GVW (320 tons) projected vertically down on the graph.

II. Drawing left to the Rimpull Graph (373.3 kN, 2nd gear).

III. Drawing down to the speed (12 km/h).

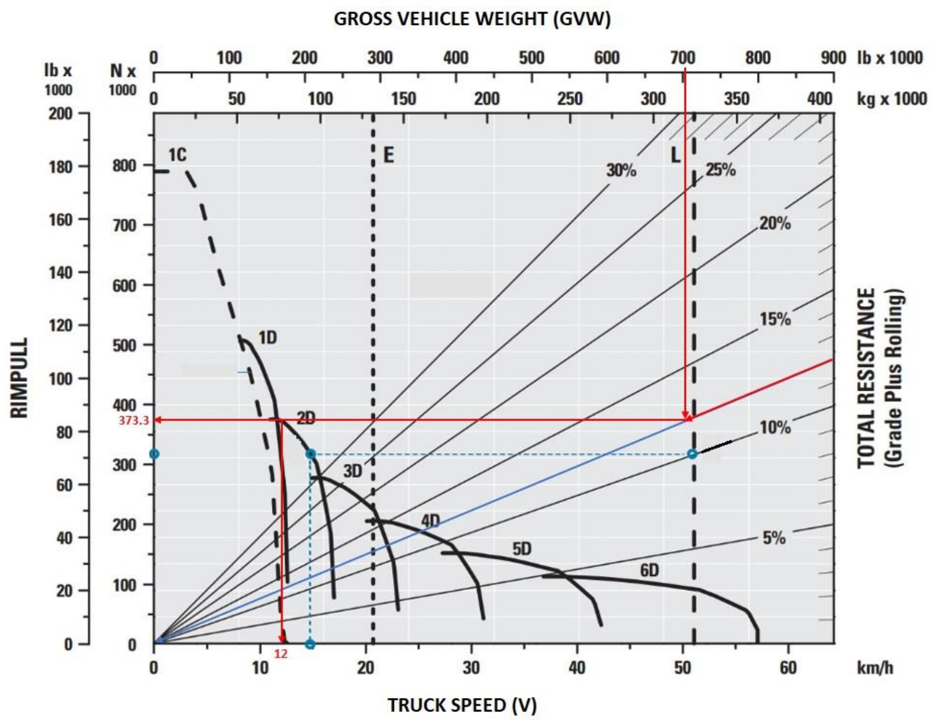

Figure 26: Rimpull Curve. Komatsu 930E-4 Operation Parameters are projected in red lines and expressed in red values. (Leiva, 2013) (Komatsu, 2013) (Komatsu, 2007).

Similarly, the Retarding Curve represented in Figure 27 is the equivalent to Rimpull Curve when the truck is moving down the road. The Retarding Curve reflects the speed for the engine gear which avoids the brakes overheating. Therefore, when the truck is going down through the road, *v* is calculated with the Retarding Curve.

Exemplifying in green lines on Figure 27, if a truck is evaluated for a GVW of 400 ton and an Effective Grade (negative GR plus positive RR) of 7.8% in module, then the truck speed would be 16 km/h.

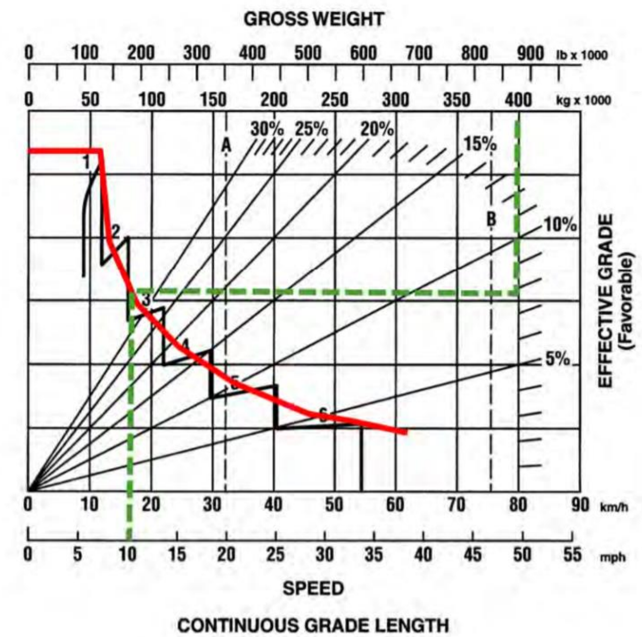

Figure 27: Retarding Curve. (Leiva, 2013)

Then, the truck hourly Fuel Consumption (FC) can be calculated from Equation 3.

$$FC = \frac{SFC}{FD} \cdot LF \cdot P$$

Equation 3: Fuel Consumption formula. (Komatsu, 2013).

In Equation 3, SFC is the engine specific fuel consumption at full power and FD is the Fuel density. LF is the engine load factor and is defined as the ratio of average payload to the maximum load in an operating cycle. And P is the truck power (in kW) calculated for the truck operation's best performance.

Finally, from Equation 4 is calculated the Komatsu 930E-4 fuel cost per hour.

$$Fuel\ Cost\ per\ hour = FC \times Local\ Unit\ Price\ of\ Fuel$$

Equation 4: Fuel Cost per hour formula. (Komatsu, 2013).

According to Komatsu 930E-4 specifications and parameters introduced in the previous equations, Table 6 summarizes values assumed for truck performance.

Table 6: Operation and Cost Parameters for Komatsu 930E-4 Electric Haul Truck. (Floche Juelsgaard, Pratt, & Magnusson Svendsen, 2020) (GlobalPetrolPrices, 2020) (Komatsu, 2007) (Rakha, Lucic, Henrique, Setti, & Van Aerde, 2001).

Parameter	Value
Diesel Density	$0.85\ \frac{kg}{l}$
2020 Local Diesel Cost	$0.62\ \frac{USD}{l}$
2030 Local Diesel Cost	$0.7\ \frac{USD}{l}$
Annual increase of Diesel Cost	2%
Specific Fuel Consumption (SFC)	$0.2\ \frac{kg}{kW \cdot h}$
Load Factor (LF)	0.35
Rolling Resistance (RR)	+ 2%
Empty Vehicle Weight (EVW)	210 ton
Gross Vehicle Weight (GVW)	290 ton
Frontal Area of Truck ($\boldsymbol{A_{ve}}$)	$64.05\ m^2$
Idling Fuel Consumption	$4.2\ \frac{l}{h}$
Road Surface Coefficient (C_r)	10
Truck Aerodynamic Drag Coefficient (C_d)	1.03
First Rolling Resistance Constant (c_1)	0.0328
Second Rolling Resistance Constant (c_2)	4.575
Gravity Acceleration (g)	$9.81\ \frac{m}{s^2}$
Air Density ($\boldsymbol{\rho_{air}}$)	$1.25\ \frac{kg}{m^3}$

For truck retrofitting, there are two cases considered into the heavy-duty mining truck retrofitted with H2 PEM fuel cell scenario. Both cases are the 2020 and 2030 truck retrofitting. The 2020 and 2030 truck retrofitting scenarios involve the technology and hydrogen costs from 2020 and 2030, respectively.

In Table 7 are represented the technology and hydrogen costs for 2020 and 2030 truck retrofitting.

Table 7: Production, Compression, Storage and Dispensing Costs, with respective H2 Onboard Storage Cost considered.

Parameter	Value $\left[\frac{USD}{kg}\right]$
2020 Local H2 Production Cost	5.9
2030 Local H2 Production Cost	2
2020 H2 Production, Compression, Storage and Dispensing Cost	7
2030 H2 Production, Compression, Storage and Dispensing Cost	3
H2 Onboard Storage Cost	500

Particularly, H2 tank capacity of Onboard Storage is specified in Table 8, with main parameters for H2 tank sizing.

Table 8: Parameters considered for H2 tank sizing.

Parameter	Value
Diesel Tank Capacity	4,542 $[l]$
Diesel Heat Value	36.64 $\left[\frac{MJ}{l}\right]$
Heat Value Capacity in Tank	166,396 $[MJ]$
H2 Tank Capacity	840 $[kg]$
Correction Factor	0.61

Where H2 Tank Capacity and Correction Factor have been calculated from Equation 5 and Equation 6, respectively.

$$H2\,Tank\,Capacity = \frac{H2\,Tank\,Capacity\,[kg\,H2]}{120\left[\frac{MJ}{kg\,H2}\right]} \cdot Correction\,Factor$$

Equation 5: H2 Tank Capacity Formula.

$$Correction\,Factor = \left(\frac{Total\,Energy\,required\,in\,Diesel\,Genset\,[kWh]}{Total\,Energy\,required\,in\,PEMFC\,[kWh]}\right)^{-1}$$

Equation 6: Correction Factor Formula.

9.2.3. Truck Power Calculation

To obtain the truck power through the entire path, the method used to calculate the power at the wheels is based on the Comprehensive Power-based Electric Vehicle Energy Consumption Model (CPEM). In fact, the truck power studied is the power at the wheels, which corresponds to the formula presented in Equation 7.

$$P_{Wheels} = \left(m \cdot a(t) + m \cdot g \cdot \cos(\theta) \cdot \frac{C_r}{1000} \cdot (c_1 \cdot v(t) + c_2) + \frac{1}{2} \cdot \rho_{air} \cdot A_{ve} \cdot C_D \cdot v^2(t) + m \cdot g \cdot \sin(\theta)\right) \cdot v(t)$$

Equation 7: Wheels Power Formula (Fiori, Ahn, & Rakha, 2016).

Although the proposed model had been destinated for particular electric vehicle calculations, the model is general and can be used for several mobile applications, like mining trucks. Enunciated by the model, the formula in Equation 7 presents m as the vehicle mass in kg, which takes EVW or GVW value depending on whether the truck is empty or loaded, respectively. Furthermore, a is the truck acceleration (in $\frac{m}{s^2}$) calculated in Equation 8, v is the truck speed (in $\frac{m}{s}$), θ is the road grade. At last, all other terms in Equation 7 are described in Table 6.

$$a = \frac{\Delta v}{\Delta \mathrm{t}}$$

Equation 8: Truck Acceleration Formula.

Specifically, it is important to note that C_r, c_1 and c_2 are the rolling resistance parameters that vary as a function of the road surface type, road condition and vehicle tire type. For the purposes of the prefeasibility evaluation, rolling resistance parameters are presented in Table 6 as constants for the entire path travelled by trucks.

9.2.4. Regenerative Braking Energy System

Due to the introduction of electrical regenerative braking, desirable braking performance not only guarantee to quickly stop the truck and maintain the traveling direction stable and controllable but recapture the braking energy as much as possible on various conditions of road.

In the regenerative braking mode, energy is recovered flowing from the wheels to the motor. Therefore, the wheels power is negative when the truck is going down through the road. Alternatively, when the truck is in traction mode going up through the road, the energy flows from the motor to the wheels. In traction mode the wheels power is positive.

Represented in Equation 9, the regenerative breaking energy recovered ($E_{Recoverable}$) is calculated using the regenerative braking energy efficiency (η_{rb}) and the total energy available to be recovered ($E_{Available}$).

$$E_{Recoverable}[kWh] = \eta_{rb} \cdot E_{Available}[kWh]$$

Equation 9: Energy recovered during braking Formula (Fiori, Ahn, & Rakha, 2016).

At the same time, $E_{Available}$ and η_{rb} are calculated as shown in Equation 10 and Equation 11, respectively.

$$E_{Available}[kWh] = P_{Wheels} \cdot \Delta t$$

Equation 10: Maximum Energy Available to be recovered during braking Formula (Fiori, Ahn, & Rakha, 2016).

$$\eta_{rb}(t) = \begin{cases} \left(e^{\frac{0.0411}{|a(t)|}}\right)^{-1}, & \forall a(t) < 0 \\ 0, & \forall a(t) \geq 0 \end{cases}$$

Equation 11: Regenerative Energy Efficiency Formula (Fiori, Ahn, & Rakha, 2016).

Represented in Equation 11, the regenerative energy efficiency at any instant *t* is expressed as a function of the truck instantaneous negative acceleration calculated in Equation 8.

9.3. Total Cost of Ownership and Operation Calculation: Comparative Scenarios

For both technologies, retrofitted and conventional truck, the truck trip methodology has been developed for the technical and economic prefeasibility evaluation.

Particularly, the truck trip evaluations are based on shift schedules. In this sense, with shift schedules the Spence mine is simulated to operate with two shifts per day of 10 hours each. The dayshift starts at 6:00 and ends at 16:00, with two hours for a meal break and shift preparations. The nightshift starts at 18:00 and ends at 4:00, also with two hours for shift preparations and meal break. The blasting is conducted once a day during the shift change. The operation results in an effective working time of 16 hours a day, resulting in 80% shift utilization.

Additionally, the interaction of haul trucks with other mine vehicles is estimated to be 5% of the total available working time. Therefore, the actual shift utilization used to build the model is 75%.

9.3.1. Trucks Trip Results for Retrofitted Technology Scenario

For the first evaluation scenario, Table 9 presents results obtained from the 1,043 trucks trip through the given closed-circuit path, considering haul trucks retrofitted with new technology. I.e., the entire fleet of electric-drive trucks have been adapted with hydrogen PEMFC and lithium-ion battery in the trucks power train.

Table 9: Route and Truck Parameters for the Retrofitted Technology Scenario.

Parameter	1st Route	2nd Route	3rd Route	4th Route	5th Route	6th Route	7th Route	8th Route
Truck Status	Empty	Empty	Empty	Loading	Loaded	Loaded	Loaded	Tipping
Road Condition	Flat Road	Downward Slope Road	Flat Road	Flat Road	Flat Road	Upward Slope Road	Flat Road	Flat Road
Height [masl]	1,759	1,695	1,695	1,695	1,695	1,759	1,759	1,759
Distance [m]	2,225.2	1,338	73.1	0	404.3	1,317.1	2,332.6	0
TR [%]	0	-8	0	0	0	11.2	0	0
Rimpull [kN]	-	-	-	-	-	315.5	-	-
Speed $\left[\frac{km}{h}\right]$	45.49	34.03	45.49	0	45.49	10	45.49	0
Time [s]	176	142	6	480	32	474	185	600
Truck Power [kW]	1,382	0	1,382	0	1,877	2,025	1,877	0
η_{rb}	-	0.679	-	-	-	-	-	-
Acceleration $\left[\frac{km}{h^2}\right]$	0	-1,375	0	0	0	6,388	0	0

Complementing results obtained in Table 9, Table 10 summarizes parameters calculated for the entire closed-circuit path (with no divisions considered for calculations).

Table 10: Parameters for general path considered in retrofitted scenario.

Parameter	Value
Cycle Time [s]	2,094
Total Wheel Energy Consumption per Cycle [kWh]	450
Daily Number of Cycles $\left[\frac{cycles}{day}\right]$	27
Daily Payload per Truck $\left[\frac{ton}{day}\right]$	2,160
Fleet Size	1,043

For carrying out the economic evaluation, there are many PEMFC and lithium-ion battery designs to choose from. The idea consists of select the best truck retrofitting configuration to fit the performance developed by the wheels power through the entire closed-circuit path.

To achieve the best configuration in both economic and technical terms, Figure 28 illustrates truck wheels power developed through the closed-circuit path drawn and the height at each point of the road. Additionally, Figure 28 shows PEMFC and Lithium-Ion Battery Powers delivered over time, which have been selected for the truck retrofitting.

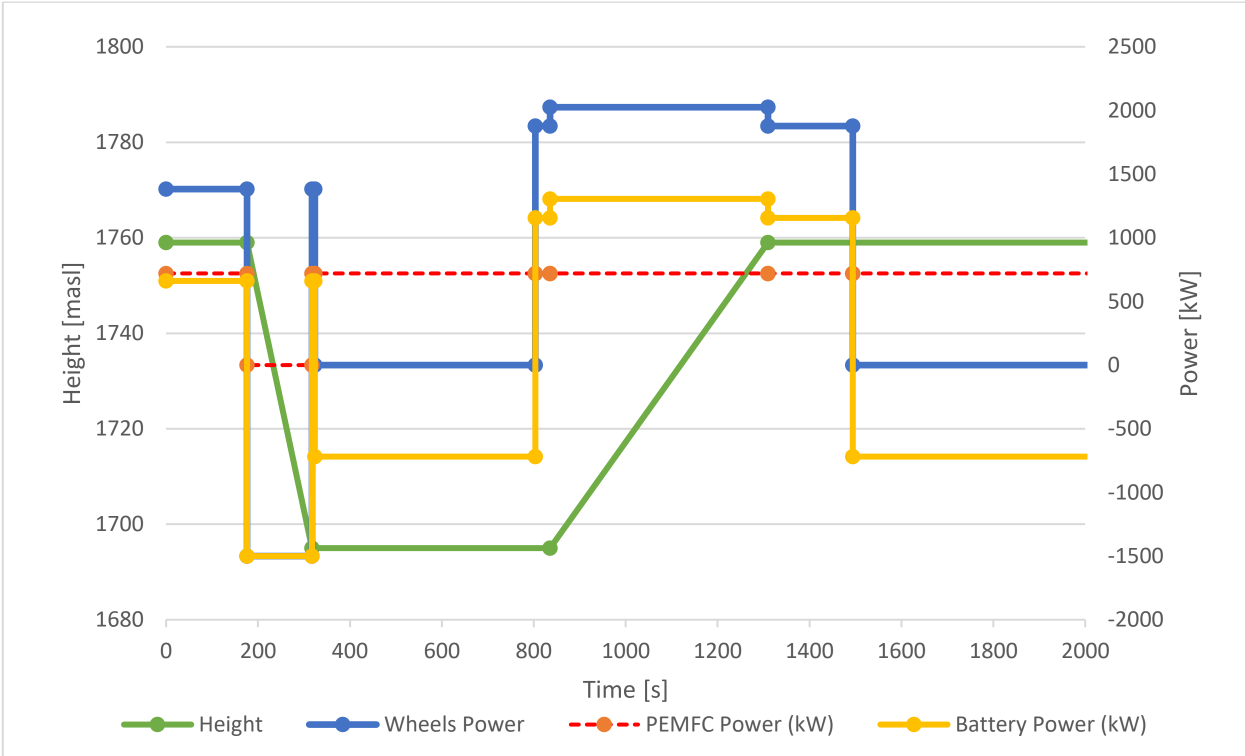

Figure 28: PEMFC, Lithium-Ion Battery and Wheels Powers projected through truck travelling time, compared with Height changes into the entire road over time.

Considering Wheels Power per cycle developed for a retrofitted truck over time and energy efficiency rates of each power train component, Figure 29 presents the energy status in every stage of the power train.

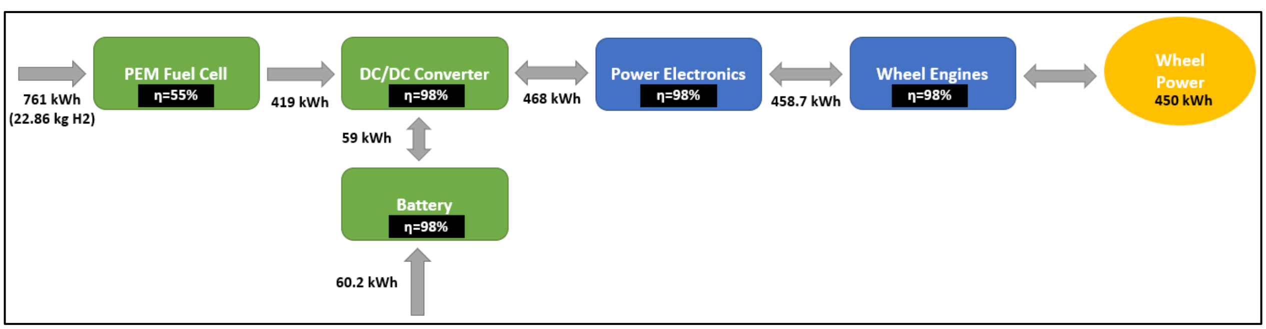

Figure 29: Power train retrofitting, with corresponding energy flows in every mechanical/electrical device.

In Figure 29, the energy generated in every stage of the retrofitted power train does not consider the degradation, the charging rate and the depth of discharge developed by the Battery.

Moreover, PEMFC and Battery always work with correction factor for efficiency loss, which have not been considered either in Figure 29.

Including all PEMFC and Battery operational parameters for correct power train sizing, Table 11, Table 12 and Table 13 show the required PEMFC and Battery size according to the required energy by the retrofitted power train.

Table 11: Required and regenerated energy parameters for PEMFC sizing.

Parameter	Value
Total required Wheel Energy [kWh]	450
Correction factor for efficiency loss	94%
Total Regenerated Energy [kWh]	59
Total required PEMFC Energy in output [kWh]	391
Total Regenerated Energy after efficiency correction [kWh]	56
Total required PEMFC Energy in output, after efficiency correction [kWh]	419

Table 12: Operational parameters for Lithium-Ion Battery sizing.

Parameter	Value
Maximum Regenerated Power Available [kW]	1,779
Usable Battery Size in end-of-life stage [kWh]	253
Usable Battery Size in end-of-life stage, after efficiency correction [kW]	269
Maximum Power Battery at 6 C-rate [kW]	1,518
Battery Degradation in end-of-life	-20%
Safety Margin (Depth of Discharge)	40%
Required Battery Size in begin-of-life stage [kWh]	470

Table 13: Energy obtained for PEMFC sizing.

Parameter	Value
Usable PEMFC Size in end-of-life stage [kW]	720
Usable PEMFC Size in end-of-life stage, after efficiency correction [kW]	765
Optimal PEMFC Load Factor	80%
Required PEMFC Size in begin-of-life stage [kW]	1,195

Considering the specific costs for commercial PEMFC and Lithium-Ion Battery, the power specifications and costs for both electrochemical devices selected are showed in Table 14.

Table 14: PEMFC and Lithium-Ion Battery selected models, costs and operational specifications.

Parameter	Value
2020 PEMFC System Unitary Cost $\left[\frac{USD}{kW}\right]$	1,706
2030 PEMFC System Unitary Cost $\left[\frac{USD}{kW}\right]$	739
2020 Lithium-Ion Battery Unitary Cost $\left[\frac{USD}{kWh}\right]$	156
2030 Lithium-Ion Battery Unitary Cost $\left[\frac{USD}{kWh}\right]$	122
Specific Proton Exchange Membrane Unitary Cost $\left[\frac{USD}{kW}\right]$	3.3
PEMFC Stack Configuration selected [kW]	1,195
Lithium-Ion Battery Configuration selected $[\boldsymbol{kWh}]$	470
2020 PEMFC Stack Cost $[\boldsymbol{USD}]$	2,039,061
2030 PEMFC Stack Cost $[\boldsymbol{USD}]$	883,593
2020 Lithium-Ion Battery System Cost $[\boldsymbol{USD}]$	73,385
2030 Lithium-Ion Battery System Cost $[\boldsymbol{USD}]$	57,391
Proton Exchange Membrane Cost $[\boldsymbol{USD}]$	4,620
Proton Exchange Membrane Lifetime Cycle $[\boldsymbol{year}]$	3
Lithium-Ion Battery Lifetime Cycle $[\boldsymbol{year}]$	2

Then, Table 15 and Table 16 summarize the 2020 and 2030 truck retrofitting's economic evaluation through clash flows calculated for 12 years, with a discount rate of 10%. Both scenarios, 2020 and 2030 truck retrofitting's economic evaluations, are analyzed for different technology and energy cost projections.

The economic evaluation considers the following items as part of the truck total cost of ownership and operation:

1. Periodic H2 Consumption
2. Periodic H2 Production, Compression, Storage and Dispensing
3. H2 Onboard Storage
4. PEMFC System Purchase at first year
5. Lithium-Ion Battery Purchase at first year
6. Periodic Proton Exchange Membrane Purchase (Replacement)
7. Periodic Lithium-Ion Battery Purchase (Replacement)
8. Fleet Size
9. Mechanical Availability

Table 15: Economic Evaluation for a 2020 Truck Retrofitting Scenario.

	Year 0	Year 1	Year 2	Year 3	Year 4	Year 5	Year 6	Year 7	Year 8	Year 9	Year 10	Year 11	Year 12
CAPEX [USD]	2,532,312	-	-	73,385	4,620	-	73,385	-	4,620	73,385	-	-	78,005
Energy Cost [USD]	1,419,088	1,419,088	1,419,088	1,419,088	1,419,088	1,419,088	1,419,088	1,419,088	1,419,088	1,419,088	1,419,088	1,419,088	1,419,088
Total [USD]	3,951,400	1,419,088	1,419,088	1,492,473	1,423,708	1,419,088	1,492,473	1,419,088	1,423,708	1,492,473	1,419,088	1,419,088	1,497,093
NPV [USD]	**12,525,888**												

Table 16: Economic Evaluation for a 2030 Truck Retrofitting Scenario.

Year	0	1	2	3	4	5	6	7	8	9	10	11	12
CAPEX [USD]	1,360,850	-	-	57,391	4,620	-	57,391	-	4,620	57,391	-	-	62,011
Energy Cost [USD]	608,181	608,181	608,181	608,181	608,181	608,181	608,181	608,181	608,181	608,181	608,181	608,181	608,181
Total [USD]	1,969,031	608,181	608,181	665,571	612,801	608,181	665,571	608,181	612,801	665,571	608,181	608,181	670,191
NPV [USD]	**5,670,826**												

For economic evaluations of 2020 and 2030 Truck Retrofitting Scenarios, Figure 30 represents a costs comparation among the most important items considered in the TCO. Analyzing Figure 30, there is a reduction of 57% between 2030 and 2020 H2 Production, Compression, Storage and Dispensing costs. At the same time, between 2030 and 2020 PEMFC System costs, the cost reduction represents a 57% as well. Lastly, the reduction between 2030 and 2020 Battery costs yields only 22%, the behavior of battery cost projection tends to be constant in time, moreover from 2030.

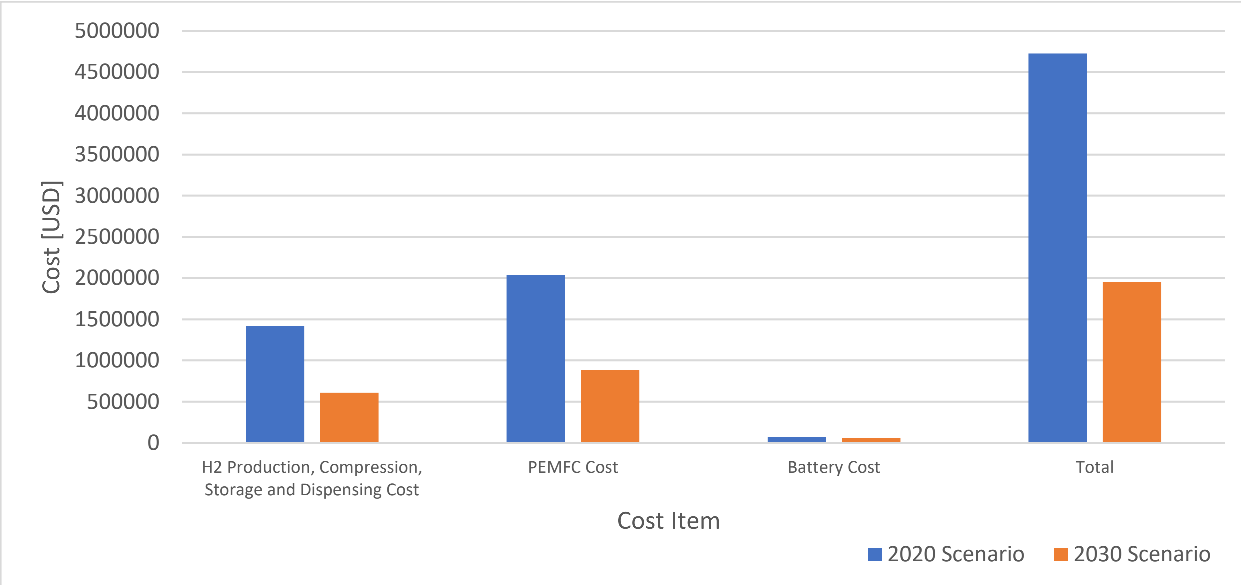

Figure 30: CAPEX and Energy Costs comparation between 2020 and 2030 truck retrofitting scenarios.

9.3.2. Trucks Trip Results for Conventional Technology Scenario

On the other hand, the second scenario corresponds to the technical and economic prefeasibility evaluation of the trucks trip through the closed-circuit path, considering 1,043 conventional electric-drive haul trucks.

In Table 17 are presented the operational parameters and results obtained from the 1,043 electric-drive trucks trip, equipped with Diesel internal combustion engines in their power trains.

Summarizing results from Table 17, Table 18 shows parameters and costs calculated for the general closed-circuit path.

Table 17: Route Parameters and Diesel consumption and costs for the conventional technology scenario.

Parameter	1st Route	2nd Route	3rd Route	4th Route	5th Route	6th Route	7th Route	8th Route
Truck Status	Empty	Empty	Empty	Loading	Loaded	Loaded	Loaded	Tipping
Road Condition	Flat Road	Downward Slope Road	Flat Road	Flat Road	Flat Road	Upward Slope Road	Flat Road	Flat Road
Height [masl]	1,759	1,695	1,695	1,695	1,695	1,759	1,759	1,759
Distance [m]	2,225.2	1,338	73.1	0	404.3	1,317.1	2,332.6	0
TR [%]	0	-8	0	0	0	11.2	0	0
Rimpull [kN]	-	-	-	-	-	315.5	-	-
Speed $\left[\frac{km}{h}\right]$	45.49	34.03	45.49	0	45.49	10	45.49	0
Time [s]	176	142	6	480	32	474	185	600
Truck Power [kW]	1,382	0	1,382	0	1,877	2,025	1,877	0

Parameter	1st Route	2nd Route	3rd Route	4th Route	5th Route	6th Route	7th Route	8th Route
Acceleration $\left[\frac{km}{h^2}\right]$	0	-1,375.2	0	0	0	6,388.2	0	0
Hourly Diesel Consumption $\left[\frac{l}{h}\right]$	113.8	0	113.8	4.2	154.6	166.8	154.6	4.2
Hourly Diesel Cost $\left[\frac{USD}{h}\right]$	70.6	0	70.6	2.6	95.8	103.4	95.8	2.6
Diesel Consumption per Route $[l]$	5.6	0	0.2	0.6	1.4	22	7.9	0.7
Daily Diesel Consumption $\left[\frac{l}{day}\right]$	150.3	0	4.9	15.1	37.1	593.2	214	19
Route Cost (considering Diesel consumption) [USD]	3.5	0	0.1	0.3	0.9	13.6	4.9	0.4

Table 18: Parameters and Costs for general path considered in the conventional technology scenario.

Parameter	Value
Cycle Time [s]	2,094
Truck Diesel Consumption by Cycle $\left[\frac{l}{cycle}\right]$	38.3
Daily Number of Cycles $\left[\frac{cycles}{day}\right]$	27
Total Cycle Cost (considering Diesel consumption) [USD]	23.7
Daily Payload $\left[\frac{ton}{day}\right]$	2,160
Daily Diesel Consumption Cost per Truck (considering all cycles) $\left[\frac{USD}{day}\right]$	640.8
Diesel Consumption Cost per ton of Mined Ore $\left[\frac{USD}{ton}\right]$	0.3
Fleet Size	1,043
Annual Diesel Consumption Cost per ton of Mined Ore (considering entire fleet size) $\left[\frac{USD}{ton}\right]$	112,936
Annual Diesel Consumption Cost (considering entire fleet size) $\left[\frac{Million\ USD}{year}\right]$	243.9

Considering Wheels Power per cycle developed for a Diesel internal combustion engine-truck over time and energy efficiency rates of each power train component, Figure 31 presents the energy status in every stage of the power train.

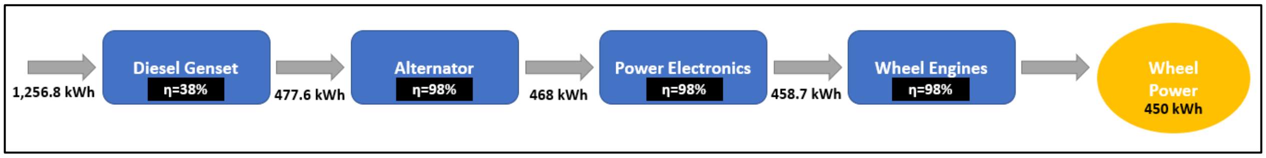

Figure 31: Conventional power train, with corresponding energy flows in every mechanical/electrical device.

Thus, for a conventional power train, the Diesel Genset considers an internal combustion engine of 1,256.8 kWh, valued at 500,000 USD for the economic evaluation.

Finally, the economic evaluation of the 1,043 electric-drive trucks, with power trains based on Diesel engines, considers the following items as part of the truck costs of ownership and operation:

1. Periodic Diesel Consumption
2. Diesel Internal Combustion Engine Purchase at first year
3. Periodic Engine Purchase (Replacement)
4. Fleet Size
5. Mechanical Availability

Additionally, for the economic evaluation, the internal combustion engine model for the Komatsu 930E-4 has a purchase cost of 500,000 USD and a lifetime cycle of 3 years.

To compare conventional technology case with the retrofitted technology one, conventional electric-drive truck is economically evaluated in Table 19 and Table 20, for 2020 and 2030 scenarios, respectively. For both 2020 and 2030 scenarios, the economic evaluation has considered a projected annual increase in Diesel cost.

Table 19: Economic Evaluation for 2020 Conventional Truck scenario (electric truck equipped with Diesel engine).

	Year 0	Year 1	Year 2	Year 3	Year 4	Year 5	Year 6	Year 7	Year 8	Year 9	Year 10	Year 11	Year 12
CAPEX [USD]	500,000	-	-	-	500,000	-	-	-	500,000	-	-	-	500,000
Energy Cost [USD]	569,177	580,561	592,172	604,016	616,096	628,418	640,986	653,806	666,882	680,220	693,824	707,700	721,854
Total [USD]	1,069,177	580,561	592,172	604,016	1,116,096	628,418	640,986	653,806	1,166,882	680,220	693,824	707,700	1,221,854
NPV [USD]	**5,570,636**												

Table 20: Economic Evaluation for 2030 Conventional Truck scenario (electric truck equipped with Diesel engine).

	Year 0	Year 1	Year 2	Year 3	Year 4	Year 5	Year 6	Year 7	Year 8	Year 9	Year 10	Year 11	Year 12
CAPEX [USD]	500,000	-	-	-	500,000	-	-	-	500,000	-	-	-	500,000
Energy Cost [USD]	642,620	655,472	668,581	681,953	695,592	709,504	723,694	738,168	752,931	767,990	783,350	799,017	814,997
Total [USD]	1,142,620	655,472	668,581	681,953	1,195,592	709,504	723,694	738,168	1,252,931	767,990	783,350	799,017	1,314,997
NPV [USD]	**6,144,668**												

9.4. Results

The comparative prefeasibility analysis for both scenarios 2020 and 2030 cases clearly show in Figure 32 the viability of investing on H2 technology, instead of the Diesel conventional technology, by 2030.

By 2020 in Chile, the high H2 production costs added to the expensive PEMFC and battery manufacturing, explain the advisability of investing in conventional Diesel engine rather than PEMFC and Lithium-ion battery for the CAEX's power train. In fact, for the conventional case, the Net Present Value (NPV) of the 2020 evaluation's cash flows is 56% lower than the 2020 retrofitted case one.

On the other hand, by 2030 in Chile the H2 technology and production costs are expected to fall due to the country potential for producing a low-cost green H2. Moreover, the PEMFC systems and Lithium-ion battery manufacturing costs are projected to fall in all the globe. So then, the total cost of operation (energy cost) and ownership (CAPEX) are expected to fall with the NPV.

In this sense, for the retrofitted case, the NPV of the 2030 evaluation's clash flows results 8% lower than the conventional case one, in the same year. Thus, in Chile, by 2030 the viability of investing in truck retrofitting of the entire fleet is higher than investing in conventional technology for all CAEX power train, in open-pit mining.

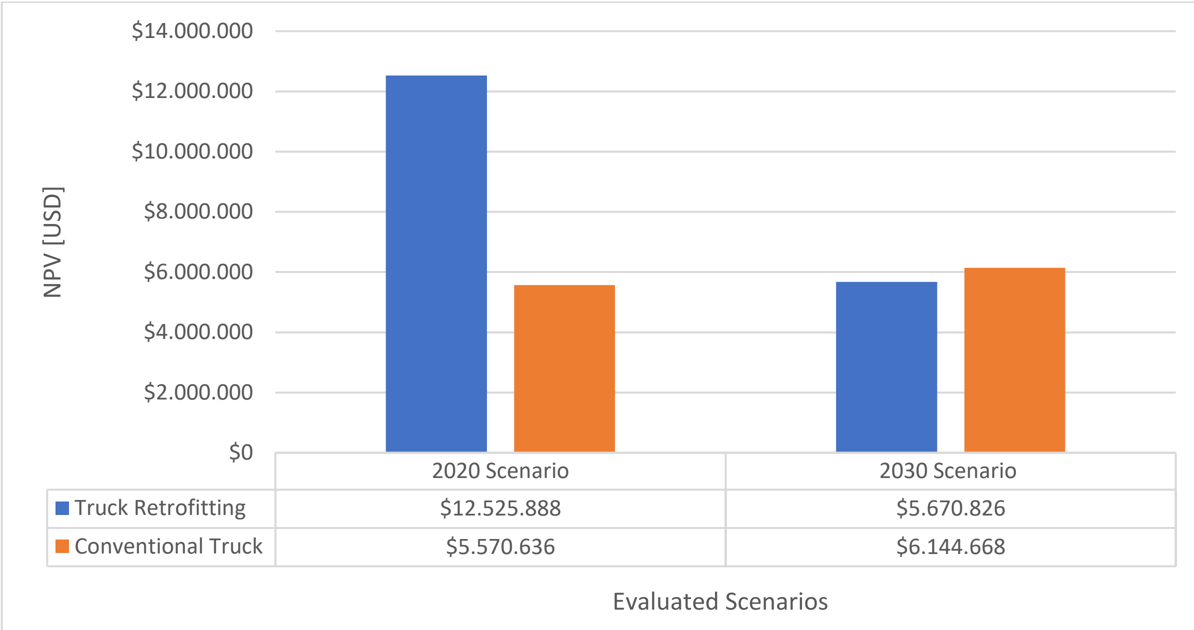

Figure 32: NPV for truck retrofitting and conventional truck cases, for each scenario of potential investment.

10. CONCLUSIONS: HYPOTHESIS AND APPROACHES

The prefeasibility study for both scenarios, the entire fleet of retrofitted CAEX and the same trucks fleet without retrofitting, shows a significant economic difference between them in 2020. The difference lies in the high current costs of the PEMFC technology. However, PEMFC purchase cost is expected to fall continuously until 2030, as long as the annual number of manufactured PEMFC systems and stacks increase over time. In fact, from the KPIs analysis is extracted that only from annual batches of the order of 100,000 manufactured PEMFC systems the purchase costs are profitable and competitive with Diesel engine purchase costs.

Additionally, performing a sensitivity analysis for H2 consumption costs, current H2 production cost causes an important impact in operational costs. In Chile, the cost of producing renewable H2 from water electrolysis varies from 5 to 6 USD/kg H2. If projections from IEA are fulfilled, when the cost of producing renewable H2 in Chile achieves 2 USD/kg the use of H2 as fuel will be economically competitive with the use of Diesel.

The prefeasibility study revealed that it is both technically and economically more viable to invest in mining CAEX retrofitted with H2 PEMFC and Lithium-ion battery in 2030 and not in 2020. For the 2020 scenario, it is economically more viable to invest in conventional CAEX equipped with internal combustion engine fueled with Diesel instead of trucks retrofitted with battery and H2 technology. However, for both 2020 and 2030 scenarios, H2 technology is technically more viable than Diesel engine, due to the current and projected higher efficiencies of fuel cells, compared with Diesel engines. Currently, the PEMFC electric efficiency is estimated in 55%, compared with the 45% of electric efficiency for Diesel engines. For the economic evaluation, the PEMFC electric efficiency is assumed to remain stable in both 2020 and 2030 scenarios under study. Thus, the higher PEMFC electric efficiency projected by 2030 could impact in the technical evaluation for the same year, which would mean a better scenario for the use of H2 PEMFC technology by 2030.

If from the costs projection is assumed that the cost per kWh produced of Lithium-Ion Battery remains relatively constant, the PEMFC cost for mobility application decreases from 1,706 USD/kW to 739 USD/kW and the green H2 production cost decreases from 5.9 USD/kg to 2 USD/kg, then by 2030 the trucks retrofitting case will be 8% more profitable than the conventional trucks case.

The most important advantage of Chile is to have huge amounts of renewable energy sources, which are also competitive in economic terms. As such, renewable H2 could be developed, contributing to the decarbonization of the Chilean energy matrix. Moreover, Chile also has the potential to become a H2 exporter on the long term, which would contribute to the global energy transition.

As mentioned before, the current lack of regulation stops manufacturers to bring H2 technologies to the country and stops integrators to deploy H2 solutions. So, the first step for the technological development of H2 within Chile consists in developing the norms and standards for H2 and its applications.

In parallel, it is important that the government promotes universities and companies to train their students/employees to obtain the required H2 skills; as well as promoting financial institutions to provide the required funding and investment mechanisms for H2 projects.

Furthermore, it is compulsory to have more technological R&D; and a collaborative platform between manufacturers, integrators and end-users, via the development of public-private partnerships and international collaboration.

Demonstrative projects should be encouraged and promoted, as part of a national H2 roadmap. The mining sector is one of the biggest energy consumers in Chile, so projects within this sector would be key to accelerate the H2 technology deployment.

In summary, H2 could become, next to copper, a key growth driver for Chile, if the correct actions are taken by the government.

11. GLOSSARY

a	Truck Acceleration
AEC	Alkaline Electrolyzer
AFC	Alkaline Fuel Cell
A_{ve}	Frontal Area of Truck
CAEX	High tonnage extraction truck
CAGR	Compound Annual Growth Rate
C_d	Truck Aerodynamic Drag Coefficient
CHP	Combined Heat and Power
CH_4	Methane
CO	Carbon Monoxide
CO_2	Carbon Dioxide
CPEM	Comprehensive Power-based Electric Vehicle Energy Consumption Model
C_r	Road Surface Coefficient
c1	First Rolling Resistance Constant
c2	Second Rolling Resistance Constant
DMFC	Direct Methanol Fuel Cell
DOE	United States Department of Energy
$E_{Recoverable}$	Regenerative Braking Energy Recovered
EVW	Empty Vehicle Weight
FC	Fuel Consumption
FCEV	Fuel Cell Electric Vehicles
FD	Fuel Density
g	Gravity Acceleration
gal	gallon
GHG	Greenhouse Gas
GR	Grade Resistance
GVW	Gross Vehicle Weight
hp	horse power
HRS	Hydrogen Refueling Station
H2	Hydrogen (Stable Hydrogen)
IC	Internal Combustion
IEA	International Energy Agency
IPPU	Industrial Processes and Products Use
kg	kilogram
kW	kilowatt
HHV	High Heating Value
LF	Load Factor
LHV	Low Heating Value
masl	Meters Above Sea Level
MW	Megawatt
MCFC	Molten Carbonate Fuel Cell
NPV	Net Present Value
N_2O	Nitrous Oxide
NPV	Net Present Value

O_2	Diatomic Oxygen
P	Truck Power
PAFC	Phosphoric Acid Fuel Cell
PEMEC	Polymer Electrolyte Membrane Electrolyzer
PEMFC	Proton Exchange Membrane Fuel Cell
r	Wheel Radius
R	Rimpull (in kg)
RF	Rimpull Force
RR	Rolling Resistance
R&D	Research and Development
s	Seconds
SFC	Specific Fuel Consumption
SOEC	Solid Oxide Electrolizer
SOFC	Solid Oxide Fuel Cell
Syngas	Synthesis Gas
T	Torque
T&D	Transmission and Distribution
TJ	Terajoules
TR	Total Resistance
TWh	Terawatt Hours
USA	United States of America
USD	United States Dollars
v	Truck Velocity
VRE	Variable Renewable Energy
W	Watt
η_{rb}	Regenerative Braking Energy Efficiency
ρ_{air}	Air Density

12. BIBLIOGRAPHY

© Caterpillar. (2020, May 21). Addressing unique challenges with drive train options for mining trucks. San Diego, California, U.S.A.

2020 CNES / Airbus. (2020, July 31). *Google Earth.* Retrieved from Google Earth Application.

Alta Ley Corporation. (2019, April 12). Gestión de Cambio Climático en la Minería del Cobre en Chile. Santiago, Metropolitana, Chile.

Alta Ley Corporation. (2019). *Hoja de Ruta 2.0 de la Minería Chilena: Actualización y consensos para una mirada renovada.* Santiago: ALTALEY.

Ballard. (2019, December 18). *© 2020 Ballard Power Systems.* Retrieved from Ballard Web site: https://www.ballard.com/about-ballard/newsroom/news-releases/2019/07/31/ballard-reports-q2-2019-results

Ballard. (2019, December 18). *© Ballard Power Systems.* Retrieved from Direct Industry Web site: https://pdf.directindustry.com/pdf/ballard/pem-fuel-cell-product-portfolio/22779-160251.html

Barrientos, V. (2018). *Operational Innovation and Mining Trucks' Tyres.* Lima.

Bloom Energy Corporation. (2018). *Annual Report on Form 10-K for the Years Ended.* California.

Bodén, A. (2016). *PowerCell Fuel Cell Stacks and Systems.* Göteborg.

Bodén, A. D. (2015). *PowerCell enables fuel cell solutions based on existing fuels.* Gothenburg.

BP. (2018). *BP Statistical Review of World Energy 2018.* London: BP p.l.c.

Bravo, S. (2018, July 13). Las emisiones de CO2 crecieron en España un 6,9% en 2017. Madrid, Alcobendas, Spain.

Ceres Power Holdings plc . (2019). *Half-yearly report for the six months ended 31 December 2018* . Crawley.

CeresPower. (2019, December 18). *© Ceres Power Holdings plc*. Retrieved from Ceres Power Holdings Web site: https://www.cerespower.com/news/latest-news/ceres-to-launch-new-fuel-cell-manufacturing-facility/

Chile Foundation. (2018, June 5). Impactos del cambio climático en el sector minero. Santiago, Metropolitana, Chile.

Climate Action Tracker. (2020, April 10). *Copyright 2020 Climate Action Tracker.* Retrieved from Climate Action Tracker Web site: https://climateactiontracker.org/countries/chile/

COCHILCO . (2019). *Informe de actualización del consumo energético de la minería del cobre al año 2018.* Santiago.

COCHILCO. (2015). *Analysis of the market for critical inputs in copper mining.* Santiago.

COCHILCO. (2016). *Copper-mining critical supplies market analysis.* Santiago.

COCHILCO. (2016). *Report about indirect GHG emissions to the year 2015* . Santiago: COCHILCO Reports.

COCHILCO. (2017). *Analysis of the market for critical inputs in copper mining (2017).* Santiago.

COCHILCO. (2017). *Update Report of direct and indirect GHG emissions in Copper Mining to the year 2016.* Santiago: COCHILCO Reports.

COCHILCO. (2019). *Analysis of the market for critical inputs in copper mining (2018)* . Santiago.

COCHILCO. (2019). *Yearbook: Copper and other Mineral Statistics 1999-2018.* Santiago: Yankovic.net.

COLLAHUASI. (2019). *2018 Carbon Footprint* . Santiago: COLLAHUASI Reports.

CORFO Government of Chile . (2017). *TECHNICAL GUIDE: Development of dual hydrogen-diesel combustion system for high tonnage mining trucks.* Santiago.

DEMCOPEM-2MW. (2019, December 18). *© Copyright DEMCOPEM-2MW.* Retrieved from DEMCOPEM-2MW Web site: https://demcopem-2mw.eu/news/nedstack-completes-stack-production-for-2-mw-power-plant/

Doosan Corporation. (2019). *Spin-off to set the stage for revaluation of in-house businesses.* Connecticut.

Doosan Fuel Cell America . (2017). *Fuel Cells: The Clean Energy You Count On.* Connecticut.

E4tech. (2018, December). *California Hydrogen Business Council ©.* London. Retrieved from CHBC Web site: https://www.californiahydrogen.org/wp-content/uploads/2019/01/TheFuelCellIndustryReview2018.pdf

E4tech. (2018). *The Fuel Cell Industry Review.* London.

Ekdunge, P. D. (2017). *H2 and Fuel Cells in maritime application.* Valencia.

European Commission. (2019). *JRC Technical Reports: Global deployment of large capacity stationary fuel cells.* Luxembourg.

EUROPEAN COMMISSION, Community Research. (2003). *Hydrogen Energy and Fuel Cells: A vision of our future.* Brussels.

Exxon Mobil Corporation. (2019). *Outlook For Energy: A Perspective to 2040.* Texas: ExxonMobil.

Ferraro, M., Sergi, F., Brunaccini, G., Dispenza, G., Andaloro, L., Briguglio, N., & Antonucci, V. (2009). *PEM Fuel Cell Systems for Distributed Energy: Actual Performance, Lifetime and Reliability of a Pure Hydrogen Pre-commercial System* . Messina.

Fiori, C., Ahn, K., & Rakha, H. (2016). *Power-based electric vehicle energy consumption model: Model development and validation.* Blacksburg: ELSEVIER.

Floche Juelsgaard, K., Pratt, J., & Magnusson Svendsen, T. (2020). *Fuel Cells: Key operational challenges.* California: Riviera.

FuelCell Energy, Inc. (2018). *2018 Annual Report.* Danbury.

FuelCell Energy, Inc. (2019, December 18). *© 2018 FuelCell Energy, Inc.* Retrieved from FuelCell Energy Web site: https://www.fuelcellenergy.com/about-us-basic/manufacturing/

FuelCellsWorks. (2019, December 18). *© 1999-2020 FuelCellsWorks*. Retrieved from FuelCellsWorks Web site: https://fuelcellsworks.com/news/fcw-exclusive-tokyo-fuel-cell-expo-2019-300000-ene-farms/

FuellCellsWorks. (2019, December 18). *© 1999-2020 FuelCellsWorks.* Retrieved from FuelCellsWorks Web site: https://fuelcellsworks.com/news/toyota-installs-stationary-fuel-cell-generator-based-on-the-mirai-fc-system-at-its-honsha-plant-in-japan/

Fuji Electric Co., Ltd. (2017). *Fuji Electric Review Vol. 63 No. 1.* Gate City Ohsaki: EGUCHI Naoya.

Fuji Electric Co., Ltd. (2019). *Fuji Electric Report FInancials 2019.* Gate City Ohsaki: EGUCHI Naoya.

GENCELL. (2019, December 18). *GENCELL ©.* Retrieved from GENCELL Market Segments: https://www.gencellenergy.com/news/comparing-fuel-cell-technologies/

GlobalPetrolPrices. (2020, July 20). *GlobalPetrolPrices.com*. Retrieved from GlobalPetrolPrices Web site: https://es.globalpetrolprices.com/Chile/diesel_prices/

GlobeNewswire. (2019, December 18). *© 2020 GlobeNewswire, Inc.* Retrieved from Newswire Distribution Network & Management: https://www.globenewswire.com/news-release/2018/11/05/1645111/0/en/FuelCell-Energy-to-Acquire-14-9-Megawatt-Bridgeport-Fuel-Cell-Park-from-Dominion-Energy.html

Hawthorne Cat. (2014). *Caterpillar® Performance Handbook - Edition 44.* San Diego.

Hidai, S. P. (2018). *Fuel Cell Productions of TOSHIBA Fuel Cell Power Systems Corp.* Tokio.

Hydrogen Council. (2017). *Hydrogen scaling up: A sustainable pathway for the global energy transition.* Brussels.

Hydrogen Council. (2018, September). *Hydrogen meets digital: New opportunities for the energy and mobility system.* Brussels. Retrieved from Hydrogen Council website: https://hydrogencouncil.com/wp-content/uploads/2018/10/Hydrogen-Council-Hydrogen-Meets-Digital-2018.pdf

Hydrogen Council. (2018). *Hydrogen meets digital: New opportunities for the energy and mobility system.* Brussels.

Hydrogenics. (2010, May 4). Using Hydrogen Energy Storage System to Enable 100% Renewable Energy in Communities. Long Beach, California, United States.

Hydrogenics. (2016). *HYPM-HD 30 POWER MODULE.* Mississauga.

INACAP. (2020, May 26). Trucks for Open-Pit and Underground Mining sectors . Santiago, RM, Chile.

INKWOOD Research . (2019, December 18). *INKWOOD RESEARCH ©.* Retrieved from INKWOOD RESEARCH Web site: https://www.inkwoodresearch.com/global-fuel-cell-market-cagr-of-16-58-by-2026/

International Energy Agency (IEA). (2015). *Technology Roadmap Hydrogen and Fuel Cells.* Paris.

IRENA. (2018). *Renewable Energy Statics 2018.* New York.

IRENA. (2019). *Hydrogen: A Renewable Energy Perspective.* Tokyo: IRENA PUBLICATIONS.

ITP Thermal Pty Limited. (2018). *Hydrogen Research & Development in South Australia.* Canberra.

Komatsu. (2007). *Komatsu 930E-4 Electric Drive Truck.* Tokyo: 2007 Komatsu Publications.

Komatsu. (2013). *Specification & Application Handbook Edition 31.* Tokyo: 2013 Komatsu Publications.

Leiva, O. (2013). *Haulage Profile - Advances in Vulcan 9.* Valparaíso .

LG Fuel Cell Systems Inc. (2013). *Overview Presentation: Hydrogen and Fuel Cell Technical Advisory Committee.* Ohio.

LG Fuel Cell Systems Inc. (2017). *LG Fuel Cell Systems Program and Technology Update: DOE 18th Annual SOFC Review.* Ohio.

LG Fuel Cell Systems Inc. (2018). *19th SOFC Annual Workshop* . Ohio.

Market Report Center. (2016). *CRE Software Market Sizing & Segmentation Report.* Boston: Inkwood Research.

MCH Chilean Mining . (2015). *Mining Equipment Survey / 2013-2014.* Santiago: © Editec S.A.

MCH Chilean Mining. (2013). *Mining Equipment Survey / 2011-2012.* Santiago: © Editec S.A.

Ministry of Environment, Government of Chile . (2011). *2nd National Comunication of Chile to the United Nations Framework Convention on Climate Change.* Santiago: RyR.

Ministry of Environment, Government of Chile. (2018). *Tercer Informe Bienal de Actualización de Chile sobre Cambio Climático 2018.* Santiago: SNICHILE.

Ministry of Environment, Government of Chile. (2019, April 12). National Determinated Contribution (NDC). Santiago, Metropolitana, Chile.

Miyake, T. (2019, December 18). *© Nikkei Business Publications, Inc.* Retrieved from Nikkei xTech/Nikkei Electronics: https://tech.nikkeibp.co.jp/dm/atclen/news_en/15mk/120302525/

Nedstack. (2019, December 18). *© Nedstack.* Retrieved from Nedstack Web site: http://test.nedstack.nl/nedstack-product-range/

Nel Hydrogen. (2020, January 20). © *2020 Nel ASA*. Retrieved from Nel ASA Wed site: https://nelhydrogen.com/about/
Nuvera Fuel Cells. (2006). *FORZATM Rail Power Module: 2nd INTERNATIONAL HYDROGEN TRAIN AND HYDRAIL CONFERENCE.* Herning.
Nuvera Fuel Cells. (2016). *Presentation Nuvera Fuel Cells.* Dallas.
Office of Energy Efficiency & Renewable Energy. (2019, December 18). *U.S. Department of Energy*. Retrieved from Energy.gov: https://www.energy.gov/eere/fuelcells/doe-technical-targets-hydrogen-production-electrolysis
Office of Fuel Cell Technologies, U.S. DOE. (2011). *Hydrogen Threshold Cost Calculation.* Washington D.C.
Panasonic. (2019, December 18). © *Panasonic Corporation.* Retrieved from Panasonic Web site: https://news.panasonic.com/global/press/data/2018/11/en181101-6/en181101-6.html
Panasonic Corporation & Viessman Group. (2019, December 18). © *Panasonic Corporation.* Retrieved from Panasonic Web site: https://news.panasonic.com/global/press/data/2013/09/en130910-4/en130910-4.html
Plug Power. (2018). *Plug Power Reports Breakthrough Fourth Quarter of 2018.* New York.
Plug Power. (2019). *Second Quarter 2019 Recap: Record Second Quarter Deployments for the Company*. New York.
Posco Energy. (2015). *Development & Deployment Status of Stationary Fuel Cells in Korea.* Seoul.
Posco Energy. (2018). *Beyond Energy, Better Life.* Seoul.
Posco Energy Company. (2019, December 18). © *poscoenergy*. Retrieved from poscoenergy Web site: http://eng.poscoenergy.com/eng/renew/_service/business/battery/product_dfc3000.asp
PowerCell Sweden AB. (2018). *Annual Report 2018.* Gothenburg.
PwC – Mining Intelligence and Benchmarking. (2013). *Truck & Loader Dictionary.* Brisbane: PricewaterhouseCoopers.
Quick, D. (2019, December 18). *Panasonic.* Retrieved from © New Atlas: https://newatlas.com/ene-farm-home-fuel-cell-panasonic/25856/
Rakha, H., Lucic, I., Henrique, S., Setti, J. R., & Van Aerde, M. (2001). *VEHICLE DYNAMIC MODEL FOR PREDICTING MAXIMUM TRUCK ACCELERATION LEVELS.* Virginia: ASCE.
Richter, A. (2009, August 8). Fuji Electric with new binary cycle plant and 50% global market share goal . (T. D. Shimbum, Interviewer)
Secretary-General of the European Comission. (2019, December 18). *EU Monitor*. Retrieved from EU Monitor Web site: https://www.eumonitor.nl/9353000/1/j9vvik7m1c3gyxp/vjzx9axjibzm
SFC Energy AG. (2018). *Annual Report 2018.* Brunnthal: SFC Energy AG/CROSS ALLIANCE communication GmbH.
SFC Energy AG. (2019). *Half-year Report Q2/2019.* Brunnthal: SFC Energy AG/CROSS ALLIANCE.
Shell. (2017). *Shell Hydrogen Study*. Hamburg.
SOLIDpower. (2016). Ene Field: Fuel Cells x Combined Heat and Power. Louisville, Kentucky, United States.
SOLIDpower. (2017, November 24). SOLIDPOWER EXPANDS ITS PRODUCTION CAPACITIES . Mezzolombardo, TN, Italy.
Soofastaei, A., Karimpour, E., Knights, P., & Kizil, M. (2017). *Energy-Efficient Loading and Hauling Operations.* Rolla, Missouri: Springer International Publishing AG 2018.

Tajitsu, N., & Shiraki, M. (2019, December 18). © *Reuters*. Retrieved from Reuters Web site: https://www.reuters.com/article/us-toyota-hydrogen/toyota-plans-to-expand-production-shrink-cost-of-hydrogen-fuel-cell-vehicles-idUSKBN1KG0Y0

The International Council on Clean Transportation. (2017). *Developing hydrogen fueling infrastructure for fuel cell vehicles: A status update.* Washington.

The Parker Bay Company. (2020, April 29). Mining Trucks. Erie, Pennsylvania, U.S.A.

Thomas, D. (2016, May). Hydrogenics Corporate Presentation & Renewable Hydrogen activities. Mississauga, Ontario, Canada .

Thompson Reuters. (2015). *Mining Equipment List 2013-2014.* Santiago.

Toshiba Energy. (2019, December 18). *Copyright © 1995-2020 Toshiba Energy Systems & Solutions Corporation.* Retrieved from Toshiba Web site: https://www.toshiba-energy.com/en/hydrogen/product/fuel-cell.htm

Toyota Boshoku. (2019). *Toyota Boshoku Report 2019.* Aichi.

Tröger, M. (2016, April 4). Hydrogenics Fuel Cell Systems for mobile Heavy Duty applications. Recklinghausen, Renania septentrional-Westfalia, Germany.

TUV SUD America Inc. (2019, December 18). © *GlobeNewswire, Inc.* Retrieved from GlobeNewswire Web site: https://www.globenewswire.com/news-release/2019/02/15/1726095/0/en/Highest-increase-of-hydrogen-refuelling-stations-in-Germany-worldwide-in-2018-again.html

TUV SUD America Inc. (2019, December 18). *GlobeNewswire, Inc.* Retrieved from GlobeNewswire Web site: https://www.globenewswire.com/news-release/2019/02/15/1726095/0/en/Highest-increase-of-hydrogen-refuelling-stations-in-Germany-worldwide-in-2018-again.html

U.S. Department of Energy . (2018). *2018 Cost Projections of PEM Fuel Cell Systems for Automobiles and Medium-Duty Vehicles.* Washington.

U.S. Department of Energy. (2016). *Fuel Cell Technologies Market Report 2016.* California.

U.S. Department of Energy. (2017). *DOE Hydrogen and Fuel Cells Program Record.* Washington.

U.S. Department of Energy Fuel Cell Technologies Office. (2017). *Hydrogen and Fuel Cells Overview.* Maryland.

U.S. Department of Energy Office of Energy Efficiency & Renewable Energy. (2018, June 13). *Hydrogen and Fuel Cell Program Overview.* Washington . Retrieved from Fuel Cell Technologies Office, DOE Energy Efficiency and Renewable Energy Web site: https://www.hydrogen.energy.gov/pdfs/review18/01_satyapal_plenary_2018_amr.pdf

U.S. Department of Energy Office of Energy Efficiency & Renewable Energy. (2018). *Hydrogen and Fuel Cell Program Overview.* Washington.

U.S. Department of Energy: Energy Efficiency & Renewable Energy. (2010). *2008 FUEL CELL TECHNOLOGIES MARKET REPORT.* Washington.

Wesoff, E. (2019, December 18). © *Greentech Media.* Retrieved from gtm: A Wood Mackenzie Business Web site: https://www.greentechmedia.com/articles/read/stationary-fuel-cell-industry-financials-2018-in-brief

Wesoff, E. (2019, December 18). © *Greentech Media*. Retrieved from gtm: A Wood Mackenzie Business Web site: https://www.greentechmedia.com/articles/read/bloom-optimistic-as-it-doubles-fuel-cell-revenue-in-2018#gs.5pdnd1

Wesoff, E. (2019, December 18). *Greentech Media* ©. Retrieved from gtm: A Wood Mackenzie Business Web site: https://www.greentechmedia.com/articles/read/stationary-fuel-cell-industry-financials-2018-in-brief#gs.5k978e

Zohuri, B. (2016). *Nuclear Energy fro Hydrogen Generation through Intermediate Heat Exchangers.* Albuquerque: Springer International Publishing Switzerland .